Carbohydrate Polymers 304 (2023) 120509

Contents lists available at ScienceDirect

Carbohydrate Polymers

journal homepage: www.elsevier.com/locate/carbpol

# Nanocellulose-based sensors in medical/clinical applications: The state-of-the-art review

Mahsa Mousavi Langari [a], Maryam Nikzad [b], Jalel Labidi [a,*]

[a] Biorefinery Processes Research Group, Chemical and Environmental Engineering Department, Faculty of Engineering, Gipuzkoa, University of the Basque Country UPV/EHU, Plaza Europa 1, 20018 Donostia, Spain
[b] Chemical Engineering Department, Babol Noshirvani University of Technology, Shariati Street, 47148-71167 Babol, Iran

ARTICLE INFO

*Keywords:*
Nanocellulose
Biosensor
Chemical sensor
Physical sensor
Healthcare monitoring

ABSTRACT

In recent years, the considerable importance of healthcare and the indispensable appeal of curative issues, particularly the diagnosis of diseases, have propelled the invention of sensing platforms. With the development of nanotechnology, the integration of nanomaterials in such platforms has been much focused on, boosting their functionality in many fields. In this direction, there has been rapid growth in the utilisation of nanocellulose in sensors with medical applications. Indeed, this natural nanomaterial benefits from striking features, such as biocompatibility, cytocompatibility and low toxicity, as well as unprecedented physical and chemical properties. In this review, different classifications of nanocellulose-based sensors (biosensors, chemical and physical sensors), alongside some subcategories manufactured for health monitoring, stand out. Moreover, the types of nanocellulose and their roles in such sensors are discussed.

## 1. Introduction

Recently, the ageing population and significant alteration in disease age have been spotlighted in many countries, making healthcare a paramount issue. On the other hand, the widespread and rapid prevalence of the COVID-19 disease has severely threatened the lives and the health of a substantial number of people. As a consequence of this global pandemic, preventing, diagnosing and treating diseases have become much more urgent demands among people to save their lives from this infectious disease (Hermawan, Amrillah, Riapanitra, Ong, & Yin, 2021; Khan, Hasan, Hossain, Ahommed, & Daizy, 2020; Zhang et al., 2021). What is referred to as a disease diagnosis is a process that consists of recognising the reason and the nature of that disease and appraising the laboratory data of patients. It should be noted that a precise and fast diagnosis is the utmost step in efficient treatment (Nagraik et al., 2021). Unfortunately, about 14 % of diseases are misdiagnosed, which causes the death of 1.5 million people. In addition to the death of a huge number of people, losses of $750 and €446 billion in the US and EU have been reported, respectively (Haick & Tang, 2021). In conclusion, addressing this problem will reduce total healthcare costs by approximately 30 % (Zheng et al., 2021).

The advent of sensing technologies has improved healthcare drastically. Indeed, this technology has given way to the development of user-friendly, economical, sensitive and tremendously accurate early detection devices (Batista, Angels Moncusi, López-Aguilar, Martínez-Ballesté, & Solanas, 2021; Javaid, Haleem, Rab, Pratap Singh, & Suman, 2021; Mbunge, Muchemwa, Jiyane, & Batani, 2021). Generally, sensors are instruments that respond to different stimuli and are deployed to recognise and measure light, sound, motions and chemicals. They are also of great importance in controlling produced goods and managing online operations in various sectors. In addition, they play a critical role in the quality control of produced goods and management (Varshney, Kumar, Singhal, & Varshney, 2022). In this paper, a narrower definition for sensors can be presented: they are analytical instruments employed for analyte recognition. Such devices are composed of a receptor, a transducer of physicochemical signals and a processor for interpreting such signals (Torres, Troncoso, Gonzales, Sari, & Gea, 2020a). The International Union of Pure and Applied Chemistry (IUPAC) categorises sensors into three sorts: biosensors, chemical sensors and physical sensors (Nadporozhskaya, Kovsh, Paolesse, & Lvova, 2022).

It is worth mentioning that the first sensing platform in medical applications, devised in the 1950s, was implemented in cardiac pacemakers (Ali, Hu, Yttri, & Panat, 2022). The aim of employing sensors in healthcare is the acquisition of medical data of individuals. Such data

* Corresponding author.
*E-mail addresses:* seyedehmahsa.mousavilangari@ehu.eus (M.M. Langari), m.nikzad@nit.ac.ir (M. Nikzad), jalel.labidi@ehu.eus (J. Labidi).

https://doi.org/10.1016/j.carbpol.2022.120509
Received 19 September 2022; Received in revised form 23 December 2022; Accepted 24 December 2022
Available online 29 December 2022

includes a variety of bio-signals (physiological parameters) and health status (Batista et al., 2021). To exemplify, blood pressure, oxygen saturation and heart rate are measured to appraise cardiovascular activity (Kang et al., 2022; Sharma, Singh, Singh, & Sharma, 2022). In addition, tracking breathing cycles (per min) and muscle movement is carried out to evaluate the respiratory rate and muscular activity, respectively (Di Nardo, Basili, Meletani, & Scaradozzi, 2022; Stankoski et al., 2022). Temperature, blood sugar and (de)hydration level, body motions and emotional states (e.g., anxiety, fatigue, depression or cortisol) are the other types of data for health appraisal (Noor Masidayu Sayed Is, Zainab Ibrahim, & Azlina Ab. Aziz, 2022; Panigrahi et al., 2022; Sabry et al., 2022; Sandys, Edwards, McAleese, O'Hare, & O'Seaghdha, 2022; Sang et al., 2022; Wang et al., 2022).

The last decade has witnessed a substantial improvement in the scope of sensing technology through the integration of nanomaterials, thanks to their extraordinary physicochemical characteristics. What is more, they are potentially applied as non-invasive diagnostic elements and can combine several modalities within one probe. However, due to their toxicological effect on the environment and human health, researchers have focused on those types of nanomaterials generated from biomaterials (Chen & Chatterjee, 2013; Golmohammadi, Morales-Narváez, Naghdi, & Merkoçi, 2017; Liu et al., 2022). Recently, the development of sensors based on such nanomaterials, mainly nanocellulose, has attracted tremendous attention in the biomedical realm for monitoring and managing human health (Ratajczak & Stobiecka, 2020; Yuen et al., 2020). Indeed, the global market for such sensors has significantly grown due to late molecular biology innovations, and it is rising dramatically, such that it is likely to reach $50 billion by 2025 (Mohankumar, Ajayan, Mohanraj, & Yasodharan, 2021). These sensors are predicted to play a crucial role in recognising pathogens, including HIV and COVID-19 (Jiang et al., 2020).

The abundant hydroxyl groups existing on the surface of nanocellulose can be modified for selective adsorption, increasing the selectivity of electrochemical sensors. Besides, the combination of nanocellulose with nanoparticles (NPs) augments their stability on the surface of the electrode and prevents them from leaching, which can increase the sensitivity of such sensors (Mahmoud, Mahnashi, Alkahtani, & El-Wekil, 2020). The integration of nanocellulose and polyaniline (PANi), having a high tendency to aggregate in aqueous media, leads to the formation of a homogeneous film and the enhancement of conductivity and mechanical properties due to strong hydrogen bonds (Liu, Sui, & Bhattacharyya, 2014). Han et al. (2019) boosted the electrochemical performance and mechanical toughness of hybrid elastomers, containing PANi and highly viscose-natural rubber (NR) through direct polymerisation of aniline on nanocellulose, distributing PANi agglomerates in NR. Likewise, the favourable interaction between nanocellulose and carbon nanotubes (CNT) has made it a promising option for generating hybrid materials with favourable conductivity and mechanical properties for designing electrochemical sensors. Indeed, the association between the $sp^2$ carbon lattice of CNT and (200) lattice planes of nanocellulose causes the alignment of nanocellulose along the tube axis of CNT, bringing the high affinity between them (Dortez et al., 2022). On the other hand, the mixture of nanocellulose and substances with optical properties (e.g. fluorophore or plasmonic NPs, like graphene quantum dots (GQDs), graphene oxide (GO) or silver NPs (AgNPs)) lead to the formation of hydrogel with great optical features. Actually, the gel matrix of nanocellulose contributes to the good dispersion and stabilisation of GO and GQDs through π-π stacking of nanosheets, improving their luminescent characteristics (Brakat & Zhu, 2021; Ruiz-Palomero, Soriano, Benítez-Martínez, & Valcárcel, 2017; Ruiz-Palomero, Soriano, & Valcárcel, 2016). Nanocellulose also reduces the agglomeration of magnetic iron oxide ($Fe_3O_4$), which improves sensors' performance and durability (Abdalkarim et al., 2021). Moreover, in the study carried out by Jung et al. (Jung et al., 2017), the injection printing of conducting electrodes on 2,2,6,6-tetramethylpiperidine-1-oxy radical (TEMPO)-oxidized nanocellulose (TONC) formed a highly sensitive pressure sensor. This sensor benefited from the piezo resistivity of the nanocellulose substrate and could detect low pressure (0.5 KPa) in a wide range (0.5–3.0 KPa) and short time (40 ms).

The term nanocellulose refers to cellulosic materials with at least one dimension in a nano scale (Klemm et al., 2021). According to the standard terms proposed by the Technical Association of the Pulp and Paper Industry (TAPPI WI 3021), nanocellulose can be divided into two major classes: (1) nanostructured materials, consisting of cellulose microcrystal (CMC) and cellulose microfibrils (CMFs), along with (2) nanofibers, comprising three subcategories of nanofibrillated cellulose (NFC), cellulose nanocrystal (CNC) and bacterial cellulose (BC), based on their structures and the applied isolation technique (Gopi, Balakrishnan, Chandradhara, Poovathankandy, & Thomas, 2019; Tavakoli, Ghasemian, Dehghani-Firouzabadi, & Mazela, 2022).

NFC, also known as cellulose nanofiber (CNF), was discovered by Turbak et al. in 1983. This type of nanocellulose consists of both crystalline and amorphous segments, whose widths and lengths are 1–100 and 500–2000 nm, respectively (Pradhan, Jaiswal, & Jaiswal, 2022). Generally, there are two approaches for NFC fabrication: top-down and bottom-up. The former, implying extraction/or isolation, is conducted by using high-shear mechanical techniques, including grinding or milling, high-pressure homogenisation, high-intensity ultrasonication, cyrocrushing and micro fluidisation (Supian, Amin, Jamari, & Mohamad, 2020). The latter is ascribed to the production of nanofibers formed into filaments/or non-woven mats utilising various spinning methods, such as electrospinning, dry spinning, solution blow spinning, wet spinning, hybrid dry-jet wet spinning and interfacial polyelectrolyte complex spinning (Kramar & González-Benito, 2022). CNC is also defined as nanocrystalline cellulose (NCC), microcrystalline cellulose (MCC) and cellulose nanowhisker (CNW)., CNC was isolated for the first time in 1947 by Nickerson and Habrle (Hu, Pu, & Sun, 2021; Vanderfleet & Cranston, 2021). CNC is produced via a top-down approach, namely, strong acid hydrolysis, which is undertaken by solid acids (cation exchange resin and phosphotungstic acid), mineral acids ($H_2SO_4$, HCl and $H_3PO_4$), organic acids (formic acid, maleic acid, citric acid and oxalic acid) or the mixture of mineral and organic acids. The aforementioned methods end in the dissolution of aromatic and amorphous segments and the remains of crystalline regions with 5–50 nm widths and 50–500 nm lengths (Lu et al., 2022; Nagarajan et al., 2021; Shi, Li, Li, Gan, & Huang, 2021).

Biocellulose and microbial cellulose are the names designated for BC, which is 20–100 nm and several micrometres in diameter and length, respectively. BC is manufactured via a bottom-up approach by oxidative fermentation in non-synthetic/or synthetic media containing a sugar source. Compared to NFC and CNC, BC is purer and possesses a higher crystallinity degree. It was synthesised by Brown et al. for the first time in 1886 (Omran et al., 2021; Oprea & Voicu, 2020; Patil et al., 2022). NFC and CNC are isolated from natural resources, including softwood, hardwood, lignocellulosic and agricultural wastes, bast fibres and grasses and marine animals, such as tunicates+. Additionally, they can be extracted from wastepaper. Conversely, BC is produced from fungi, algae (*Valonia* and *Chaetomorpha*), invertebrates and some bacteria (*Gluconacetobacter*, *Sarcina*, *Agrobacterium*, *Acetobacter*, *Acanthamoeba* and *Achromobacter*) (Ghasemlou, Daver, Ivanova, Habibi, & Adhikari, 2021; Kumar, Rai, Gahlyan, & Kumar, 2021; Nehra & Chauhan, 2021; Oprea & Voicu, 2020; Torres, Troncoso, Gonzales, Sari, & Gea, 2020b).

Nanocellulose is utilised in a wide range of applications, from reinforcing substitutes to sensing materials in different areas, including environmental conservation, curative controls and nanomedicine, including drug delivery (Soriano & Dueñas-Mas, 2018). What has made nanocellulose a promising substance for biomedical applications is its convertible chemical features, dimensional similarity to biomolecules, non-animal origin, viscoelastic characteristics and chemistry, as well as its cytocompatibility, biocompatibility and low toxicity (Bacakova et al., 2020; Subhedar, Bhadauria, Ahankari, & Kargarzadeh, 2021). It is

worthwhile knowing that nanocellulose-based materials generally exhibit excellent mechanical, thermal, chemical, physical and barrier properties and are inert chemically (Reshmy et al., 2020). Regarding the intended applications, different modifications can be conducted on the surface of nanocellulose enriched with hydroxyl groups by introducing special functional groups. The modification methods applied to develop sensors are esterification (Wang et al., 2022), silylation (S. Zhu et al., 2021), oxidation (Yu, Hu, Guan, Zhang, & Gu, 2020), amidation (Lu et al., 2020), polymer grafting (Anirudhan, Deepa, & Binussreejayan, 2018), sulfonation (Zhao et al., 2022), etherification (Song & Rojas, 2013) and urethanisation (Wang et al., 2018).

So far, several review papers have been published in the field of nanocellulose-based sensing platforms (Dai et al., 2020; Golmohammadi et al., 2017; Nguyen, Naficy, Chandrawati, & Dehghani, 2019; Soriano & Dueñas-Mas, 2018; Teodoro et al., 2021). In these papers, after a general overview of nanocellulose types, production and/or properties, the application of such sensors in various areas (e.g., medical, environmental and food industries for detecting glucose, gas, urea, pressure, humidity, etc.) has been discussed simultaneously. What is more, there are some review papers devoted to nanocellulose application in sensors working on a foundation of one specific detection method (Zhang et al., 2020) or belonging to one category of sensor (Horta-Velázquez & Morales-Narváez, 2022; Torres et al., 2020a). Nevertheless, to the best of the authors' knowledge, there is by no means a review paper exclusively dedicated to all the classifications of nanocellulose-based sensors, including biosensors and physical and chemical sensors that function based on different detection methods in solely medical applications. The objective of this review is to address this issue. Moreover, the role and the type of nanocellulose and the mechanism of detection are highlighted.

## 2. Biosensors

Based on the latest trend in selective quantitative and semi-quantitative monitoring of biological analysis, biosensors have boosted point-of-care and real-time diagnosis, owing to their portability and ease of use (Torres et al., 2020b). These kinds of sensors, in which the receptors are mainly enzymes, antibodies, living cells or nucleic acids, convert the concentration of analytes in body fluid, such as urine, sweat, saliva and tears, as well as blood, into measurable signals. Indeed, they combine biological components with a physicochemical detector (Liu, Bao, & Wang, 2022; Mandpe, Prabhakar, Gupta, & Shende, 2020; Subhedar et al., 2021; Yoon et al., 2020). Biosensors suffer vulnerability to even negligible changes in temperature, pH and chemical environment and, in most cases, non-reusability. However, taking some measures for improving the sensitivity, response range and time of biosensors has led to their evolution over the years. For instance, the exploitation of nanomaterials in biosensors to ameliorate their performance, the augmentation of the active surface area and the decrease in the size of the sensing element have contributed to the advent of biosensors as efficient diagnostic devices (Dejous & Krishnan, 2021). Different nanomaterials, mainly NPs, nanorods, nanowires (NWs) and thin films composed of nanocrystalline components, were used in the biosensors and exhibited high sensitivity, mechanical and chemical properties (Misra, Acharya, Sushmitha, & Nehru, 2021; Nsabimana et al., 2019; Sha & Badhulika, n.d.; Shao & Xiao, 2020). Nanocellulose, featuring a fibrous matrix, has also been regarded as an ideal nanomaterial for the immobilisation of the biomolecules, such as enzymes aimed at creating biosensors with notable resilience, transparency and stability. Actually, their outstanding properties, namely showing biocompatibility, being physiologically inert and having amphiphilicity have made them promising candidates for such applications (Gennari, Führ, Volpato, & Volken de Souza, 2020; Nehra & Chauhan, 2021; Subhedar et al., 2021).

### 2.1. Biomarker sensors

Biomarkers are substances, such as sugars, electrolytes, proteins, metabolites, acids and hormones, which are measured in a biological system and carry meritorious data for analysing genetic disorders and infectious diseases. According to the definition established by the Food and Drug Administration (FDA) and the American National Institutes of Health (NIH), biomarkers could be indicators for the evaluation of the pathological process, normal biological processes and the body's response to drugs through changes in their content. Different types of biomarkers include physiologic, histologic, radiographic and molecular characteristics (Steckl & Ray, 2018; Subhedar et al., 2021; Wang et al., 2022). A great deal of research has been devoted to designing sensors containing nanocellulose for detecting several biomarkers. Some of the most recent ones are outlined in the following subsections.

#### 2.1.1. Glucose sensor

Glucose, affecting the physiological homeostasis system in living organisms, is the necessary source of energy for all cells. However, the excessive amount of it in the blood plasma has adverse effects on the kidney, cardiac system and eyesight, so monitoring and controlling the glucose content in body fluids is imperative (Li et al., 2021; Tracey et al., 2020). There are four generations of glucose sensors that function differently. The first three generations are dependent on the existence of enzymes, whereas the last one depends on catalysts for oxidising glucose. Compared with enzymatic glucose sensors, non-enzymatic ones have exhibited more satisfactory performance in terms of detection limit, cost, sensitivity, rapidity and reversibility (Tian et al., 2022). Several studies were dedicated to developing sensors for glucose detection. In this context, reasonable, stable, highly sensitive and selective non-enzymatic glucose sensors were devised via simple methods. Saikia and Karak (Saikia & Karak, 2020) produced a fluorescent nanohybrid through in-situ polymerisation of aniline in the presence of CNF and carbon dots (CD) for the detection of glucose in the 0.1 $mol.L^{-1}$ phosphate buffer solution (PBS) with at least 8 $\mu mol.L^{-1}$ concentration. To prepare the bio-based nanocomposites, various contents of nanohybrids were added to hyperbranched epoxy, which consists of sorbitol, monoglyceride of castor oil and conventional reactants. The fabricated nanohybrid and nanocomposites possessed the same limit of detection (LOD). However, nanocomposites were more stable and tolerant in chemical media according to this order: NaCl> HCl > NaOH> water. The superior hemocompatibility with mammalian blood and better biodegradability of these nanocomposites from bio-based CNF were verified using anti-haemolytic studies and optical density curves, respectively. Additionally, the thermosetting nanocomposites exhibited extraordinary mechanical and thermal properties. In this work, the interactions between hydroxyl groups of CNF and polar functional groups of CDs with amine group in aniline led to the uniform polymerisation of aniline. Moreover, CNF, PANi and CD synergistically affected the stability, sensitivity and selectivity towards glucose. Tracey et al. (Tracey et al., 2020) developed hybrid systems for sensing glucose in saliva and sweat based on nanocellulose and $Fe_3O_4$. x-CNC-$Fe_3O_4$ (x = sulphated (S) and non-sulphated (N)) was the name given to the sensing systems. Herein, CNC was considered a support for magnetic NPs that acted catalytically. The performance of the fabricated systems was assessed in the mixture of 2,2′-Azino-bis(3-ethylbenzothiazoline-6-sulfonic acid) diammonium salt (ABTS), glucose oxidase (GOx) and glucose. The obtained results revealed that both sensors had the same LOD. Fig. 1(a, b) depicts the structure of the sensors and the mechanism of colour change in them when in contact with glucose. The reaction between GOx and glucose was conducive to the production of hydrogen peroxide ($H_2O_2$), further reacting with ABTS and $Fe_3O_4$. Through the oxidation of ABTS, the colour of both sensors turned blue. In this reaction, $Fe_3O_4$ acted as a catalyst similar to horseradish peroxidase (HRP), which was employed in the sensor later invented by Neubauerova et al.. Neubauerova et al. (2020) introduced the first nanocellulose-based colourimetric biosensor

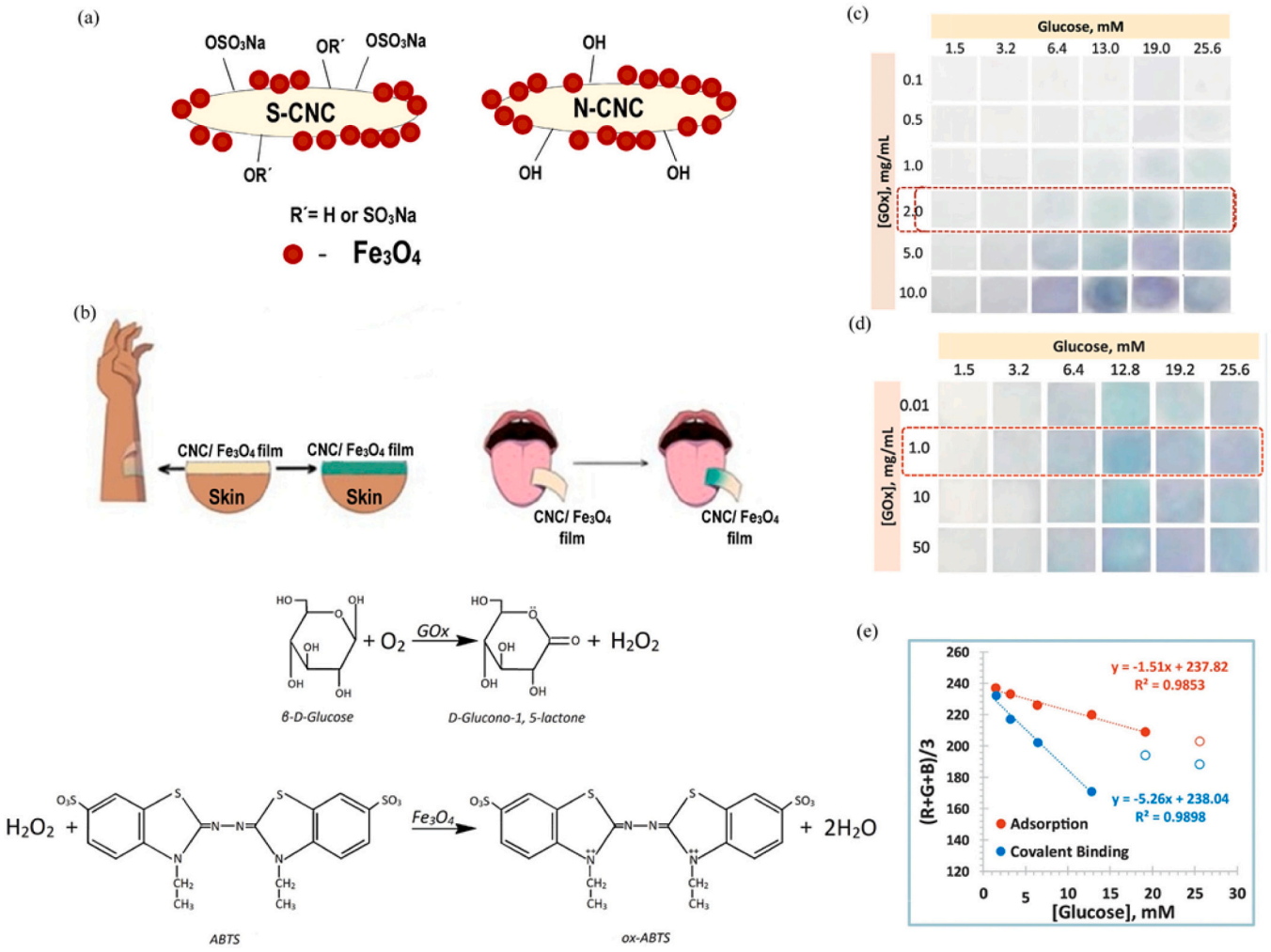


**Fig. 1.** (a) Schematic of the fabricated x-CNC-$Fe_3O_4$ platform. (b) The colour change of the sensor in contact with saliva and sweat, as well as the mechanism of this colour change (Tracey et al., 2020); digital images of the test strips, containing different concentrations of GOx: (c) covalently bounded and (d) adsorbed, respectively, in the presence of various glucose concentrations; (e) analytical calibration curve depicting the coordination of the colour against glucose concentrations (Neubauerova, Carneiro, Rodrigues, Moreira, & Sales, 2020).

for the diagnosis of glucose in urine samples through the integration of GOx on the carboxylated-nanocellulose (C-NC)/cellulose substrate, in which C-NC, produced via the oxidation of MCC using several TEMPO/hypochlorite ratios, was deposited on the cellulose paper strips. Further, different concentrations of GOx were integrated into the obtained strips from the previous stage through two distinct methods of covalent binding and adsorption. The cellulose substrate interacted with GOx through only hydrogen bonding, while cellulose doped with C-NC possessed multiple carboxyl groups, ending in intensifying the hydrogen bonding and establishing ionic interactions with positive points on the surface of GOx. The response of both sensors against various concentrations of glucose was investigated in the presence of ABTS and HRP, and the results are illustrated in Fig. 1(c, d). The colour of the resultant test strips turned blue upon reacting with glucose, similar to the sensor invented by Tracey et al. (Tracey et al., 2020), and the intensity of the colour increased with the increase in glucose concentration. In addition, the sensor containing covalent immobilisation exhibited more intense colours, which was indicative of a more sensitive response. As can be seen in Fig. 1(e), the slope of this sensor was 3.5 times sharper, proving this claim. The proposed sensor will be a viable device for the recognition of an assortment of analytes in food, environmental and medical applications. Another biosensor where nanocellulose was used for enzyme immobilisation was suggested by Tang et al. (Tang et al., 2020) to monitor cell culture. In this work, CNC acted as a matrix for GOx immobilisation and stabilisation to create a screen-printed glucose sensor with remarkable characteristics.

### 2.1.2. *Cholesterol sensor*

Cholesterol, a sterol mainly synthesised in the liver, plays a significant role in the synthesis of some vital organic molecules, including vitamin D, steroid hormones and bile acids. Despite the vitality of cholesterol in the human body, there is a borderline that the amount of this biomarker must not exceed it because the person has cardiovascular disease. As a result, several biosensors have been established to identify this biomarker and eliminate conventional cholesterol sensors' drawbacks. For instance, conventional sensors are time-consuming and require expensive device set-up, sample preparation and skilled operation (Narwal et al., 2019). Anirudhan et al. (2018) constructed an electrochemical sensor via a multi-step process using the molecular imprinting (MIP) technique. MIP involves the reversible interactions between functional monomers and a template, polymerisation and removing the template. In this study, nanocellulose, impregnated with zinc oxide (NC-ZnO), was modified through graft-copolymerisation with allyl amine and itaconic acid (IA), subsequently modified with silylated GO (Si-GO) through grafting. Finally, it was drop cast on a glassy carbon electrode (GCE). The efficiency of this sensor for the electrochemical

recognition of cholesterol was examined separately using cyclic voltammetry (CV) and differential pulse voltammetry (DPV) via ferric-ferrous-redox reaction. The selectivity of this sensor was evaluated in the existence of glucose, allylamine, uric acid (UA) and acetaminophen (AP). Among these biomolecules, AP and UA demonstrated negligible interference. The comparison between the real sample analysis through the present and the traditional methods indicated that they are consistent with each other. However, results gained from the DPV method were more precise, with a lower relative standard deviation (RSD). On the other hand, the optimum pH and response time were calculated at 7.4 (equal to the blood pH) and 10 min, respectively. Although these results proved the suitability of this sensor for analysing blood samples, the enhancement of cholesterol specificity should be the aim of future works. For this reason, the enzymatic biosensor has attracted attention owing to its great specification and selectivity features. Abdi et al. (2019) made a highly sensitive and stable electrochemical cholesterol biosensor through the immobilisation of cholesterol oxidase (ChOx) on the PANi/CNC/ionic liquid (IL)/glutaraldehyde (GLU)-modified screen-printed electrode (SPE). The fabrication process of this biosensor is depicted in Fig. 2(a). The operational conditions (the amount of PANi/CNC nanocomposite, GLU cross-linker, IL, enzyme loading, pH and buffer capacity) were optimized using response surface methodology, aiming to achieve the biosensor with a maximum sensitivity of 35.19 μA.(L.mmol$^{-1}$).cm$^{-2}$ in this study. In Fig. 2(b), the sensitivity of the biosensor (current response) to the cholesterol concentration alterations from $10^{-7}$ to 1.4 × $10^{-4}$ mol.L$^{-1}$ is exhibited. This biosensor demonstrated satisfactory reusability (RSD ≤ 3.76 %), repeatability (RSD ≤ 3.31 %) and selectivity towards cholesterol in the combination of ascorbic acid (AA), UA and glucose. The porous structure of CNC, along with the electrochemical properties of IL and PANi influenced the electrocatalytic feature of nanocomposite and synergistically changed it into a suitable host for biomolecules. The aforementioned characteristics of the proposed biosensor made it a viable option for cholesterol recognition in food industries and medical diagnostics. Although possessing considerable surface resistivity ($10^{11}$–$10^{15}$ Ω.sq.$^{-1}$) at 20–40 % relative humidity, cellulosic materials are appropriate candidates for producing conductive papers that can be used in sensors (Ragazzini et al., 2021).

### 2.1.3. Amino acid sensor

Some amino acids, such as cysteine (Cys), glutathione and cysteamine are mentioned as biological thiols. They have a crucial role in human health, and their excessive amount or deficiency in the human body can cause severe diseases. So qualitative and quantitative analyses of them are necessary for human health (Xiang, Li, & Liu, 2019). The incorporation of radiometric fluorescence (RF) sensing materials with cellulose-based materials as substrates is highly regarded as leading to the preparation of disposable, portable and low-cost sensors.

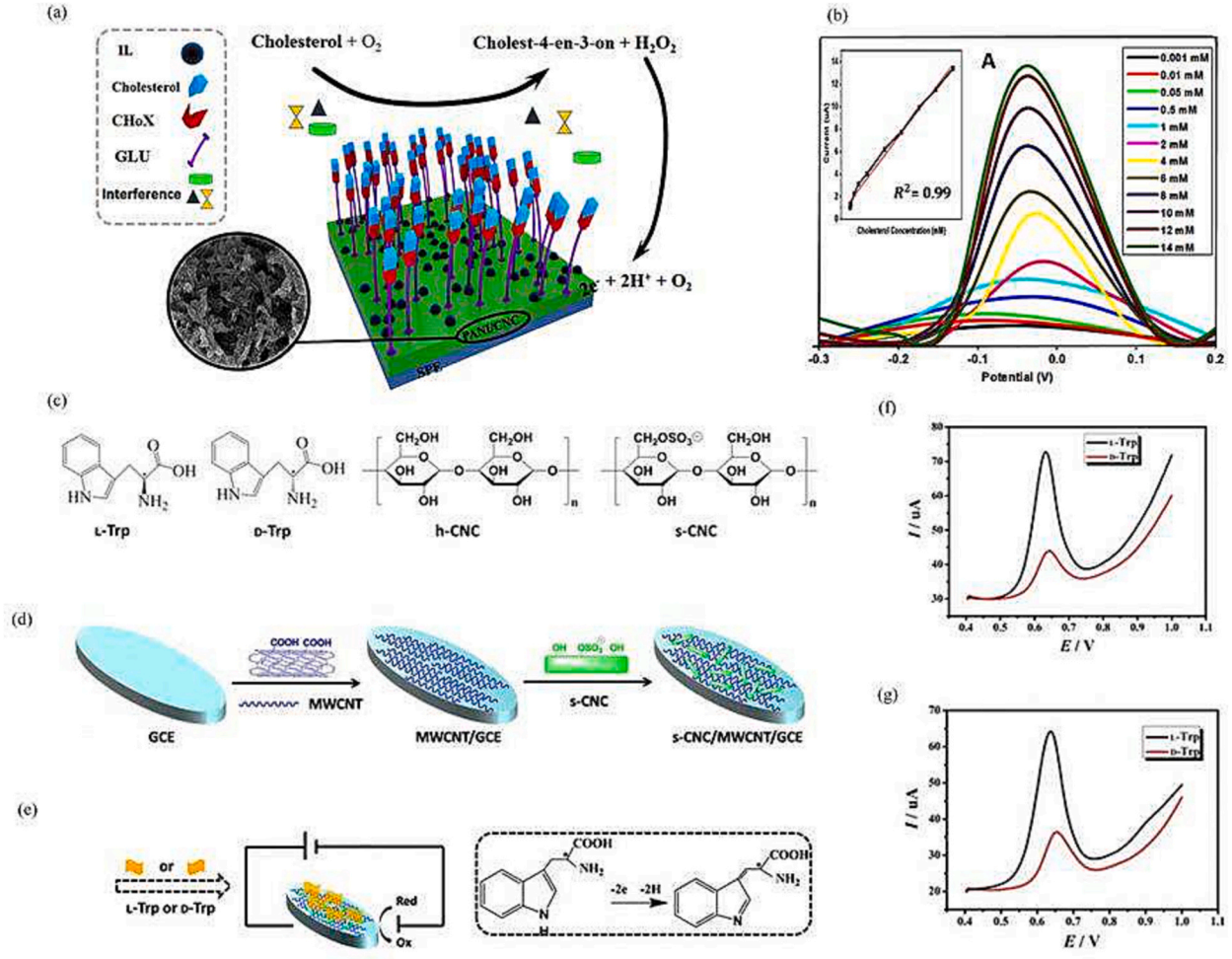


**Fig. 2.** (a) Schematic of the fabrication process of PANi/CNC/IL/GLU/ChOx-modified electrode; (b) linear relation of DPV peaks of the modified electrode against the current in a $10^{-7}$-1.4 × $10^{-4}$ mol.L$^{-1}$ concentration range of cholesterol (inset: calibration plot of current against the $10^{-7}$-1.4 × $10^{-4}$ mol.L$^{-1}$ concentration range of cholesterol) (Abdi et al., 2019); (c) chemical structures of L-Trp, D-Trp, h-CNC and s-CNC; (d) schematic of the preparation procedure of s-CNC/MWCNT/GCE nanocomposite; (e) DPV test was done on the sensing electrodes in the presence of L-Trp and D-Trp; DPV peaks of (f) s-CNC/MWCNT/GCE and (g) h-CNC/MWCNT/GCE against the current in 0.5 mmol.L$^{-1}$ of L-Trp and D-Trp (at pH 7.0 and 25 °C) (Y. Zhang et al., 2018).

Considering this fact, Abbasi-Moayed et al. (Abbasi-Moayed, Golmohammadi, Bigdeli, & Hormozi-Nezhad, 2018) prepared a sensor array for visual discrimination between the aforementioned amino acids in the mixture of various amino acids both individually and simultaneously. In this study, BC was used as a substrate for RF sensing materials; specifically, red CdTe QDs-CDs (RQDs-CDs) and *N*-Acetyl L-Cys capped green CdTe quantum dots-Rhodamin B (GQDs-RhB). It is noteworthy that this sensor could distinguish between such amino acids in human plasma. Tryptophan (Trp) is a kind of essential amino acid directly related to hepatic disease. Electrochemical discrimination of L-Trp and D-Trp as Trp enantiomers was fulfilled by the chiral sensor invented by Zhang et al. (Zhang et al., 2018). Natural polysaccharides, such as CNC, show the chiral sensing capability towards various enantiomers in electrochemical sensors. In this study, CNCs were isolated from cotton linter via two distinct processes, using $H_2SO_4$ and HCl and then designated as s-CNC and h-CNC, respectively. The obtained CNCs, carrying different groups and charges on their surface, had distinctive interactions with L-Trp and D-Trp. The chemical structures of Trp enantiomers and CNCs are illustrated in Fig. 2(c). In the next step, GCE was modified with CNCs and multi-walled CNT (MWCNTs) (Fig. 2(d)). At pH = 7 and $T = 25\ ^{\circ}C$, as an optimum condition, s-CNC/MCNT/GCE and h-CNC/MCNT/GCE nanocomposites demonstrated the peak current ratio of L-Trp 3.5 and 3 times as high as D-Trp, respectively. Fig. 2(e–g) demonstrates the DPV test performed on the nanocomposites and the results obtained from them. Overall, in this chiral sensing platform, CNCs provided selectivity towards Trp enantiomers, whereas MWCNTs were liable for the amplification of electrochemical signals owing to their conductivity. Indeed, the deposition of CNCs and MWCNTs on GCE created an interwoven network construction with cavities, which resulted from hydrogen bond interactions and physical combination and led to the recognition sites for Trp enantiomers. Cellulose-based materials are used as stabilisers for NPs, preventing them from aggregation and enhancing their fundamental features (Hu, Wu, Wang, Wang, & Zhou, 2019). In this regard, Yu et al. (Yu et al., 2020) fabricated a biosensor for L-Cys detection. To fabricate this platform, firstly, CNF was isolated from bleached wood pulp utilising TEMPO-mediated oxidation and mechanical blending. Eventually, a CNF-AgNPs suspension was prepared as a colourimetric biosensor via stabilising AgNPs on CNF through the reduction process. The aldehyde and hydroxyl groups of the CNF surface were utilised as reducing agents, whereas the carboxyl groups functioned as stabilisers for AgNP synthesis and stabilisation on the surface of CNF. The optimum condition for the recognition of L-Cys (1 $mmol.L^{-1}$) utilising CNF-AgNPs was determined through varying ionic strength (NaCl concentration) and reaction time. While the concentration of NaCl increased, the colour of the mixture of sensor and L-Cys changed from yellow to dark purple. According to the absorption spectra collected from ultraviolet-visible (UV–Vis), the optimum ionic strength and reaction time were calculated at 600 $mmol.L^{-1}$ and 5 min, respectively. At the ionic strength of 600 $mmol.L^{-1}$, the addition of L-Cys, unlike other 20 amino acids, ended in the red shift of the AgNPs SPR band and the colour change of the CNF-AgNPs because of the interaction between L-Cys and AgNPs. Indeed, the importance of measuring the level of L-Cys is because this non-essential amino acid is responsible for protein synthesis, detoxification and metabolism in the human body, and its insufficiency will cause health problems. Likewise, the determination of glycine (Gly), the simplest and smallest amino acid in cellular structures, is clinically important. Nonetheless, this component is required for vital reactions in the human body and has a key role in immunity, metabolism and cytoprotection systems, and its excessive uptake in cancer cells extends their growth. Hosseini et al. (Hosseini, Iraji Zad, Vossoughi, & Kalantarian, 2020) manufactured a sensor capable of sensing Gly through spin coating CNF on quartz crystal (QC) as a piezoelectric material demonstrating resonant frequency. CNF boosted the wettability of the QC alongside the enhancement of its surface area to host Gly molecules. In this sensing platform, CNF acted as a sensing film, not requiring further surface modification for Gly diagnosis since Gly alone interacted with CNF through hydrogen bonding and was detected. To optimise sensing functionality, different numbers of CNF layers were deposited on QC, and resonance frequency shifts were estimated before and after 1000 $\mu g.ml^{-1}$ Gly recognition. Two layers of CNF coatings showed the highest sensitivity to Gly. Afterwards, the optimum platform was used for sensing Gly in a broad range of (3–1000 $\mu g.ml^{-1}$).

#### 2.1.4. Hormone sensor

Dopamine (DA), as a neurotransmitter, plays various roles in human brains. The determining factors in cognitive functions localise in brain dopamine, whose concentrations vary from 10 $nmol.L^{-1}$ to 1 $\mu mol.L^{-1}$. The construction of sensors able to detect nanomolar amounts of this hormone in the presence of interfering compounds (e.g., UA and AA) at their physiologically proper concentrations is important. Durairaj et al. (2019) designed an ultrasensitive and selective dopamine sensor based on a modified tetrahedral amorphous carbon (ta-C) electrode by nanocomposite, which was composed of dispersed MWCNTs in a mixture of sulphated NFC (SNFC) and Nafion. Negative charges on the surface of SNFC contributed to dispersing MWCNTs in the composite, and Nafion acted as a binder to attach the composite to hydrophobic ta-C electrodes. The resultant sensor showed the LOD of 65 $nmol.L^{-1}$ in PBS and 107 $nmol.L^{-1}$ in the presence of 500 $\mu mol.L^{-1}$ UA and 1 $mmol.L^{-1}$ AA by use of 100 $mV.s^{-1}$ CV measurement. Artificial sensing membranes established based on MIP are considered a decent scaffold for wearable sensors that can monitor analytes in sweat. Mugo et al. (Mugo & Alberkant, 2020) prepared a wearable cortisol sensor via the layer-by-layer (LBL) assembly method. Cortisol is a steroid hormone in the body that plays a key role in mental health. This sensor had a fast response (3 min) and possessed acceptable reusability (RSD = 2.6 %) and supreme specificity in sweat containing glucose, epinephrine, β-oestradiol and methoxyprogestrone, among others. The base layer consisted of stretchable polydimethylsiloxane (PDMS) and other layers composed of MIP poly (glycidyl methacrylate-co ethylene glycol dimethacrylate) (poly(GMA-*co*-EGDMA)) deposited on CNC/CNT conductive nanoporous films. In comparison to other diagnosis systems, MIP presents considerable selectivity for capturing the analytes and superb thermal, chemical and mechanical stability within a broad range of operational conditions.

#### 2.1.5. Urea sensor

Urea, existing in urine and blood, is engendered by amino acid and protein breakdown. A specific amount of urea is excreted through urination daily, and a high level of it in the blood brings uraemia and kidney failure (Nwosu, Saliu, Oyinlola, & Ojo, 2020). Urease enzyme immobilisation is applied in developing urea sensors since the utilisation of enzymes, compared to traditional chemical catalysts, is more environmentally friendly and provides more specificity for the sensor (Tamaddon & Arab, 2019). Enzyme immobilisation is conducted through cross-linking, adsorption and covalent bonding. Among mentioned methods, covalent bonding engenders a more stable and robust bond. Wan Khalid, Heng, and Arip (2018) created an electrochemical urea sensor that worked on a foundation of the performance of methylene blue (MB) as a redox mediator, in responding to pH changes induced by urea hydrolysis with urease. As illustrated in Fig. 3(a–c), the fabrication of this sensor was done through the LBL method. The first two layers were made by the drop deposition of reduced GO (rGO) on SPE. Then, urease was immobilised on TEMPO-oxidized CNC (TOCNC) using N-hydroxy succinimide (NHS) and N-(3-dimethylaminopropyl)-N′- ethyl carbodiimide hydrochloride (EDC), subsequently mixed with poly(2-hydroxyethyl methacrylate), polyHEMA, and cast on rGO/SPE electrodes. Lastly, MB was drop deposited on modified electrodes. This biosensor responded to urea linearly within 0.001–0.100 $mmol.L^{-1}$ ($R^2$ = 0.9693). Nowadays, colourimetric diagnostic devices have gained remarkable attention, as they are fast, cheap, highly sensitive, simple, can be recognised with the naked eye and do not need any complex tools (Khattab et al., 2018). In this context, later, Tamaddon and Arab (2019) manufactured a colourimetric urea sensor based on the covalent binding

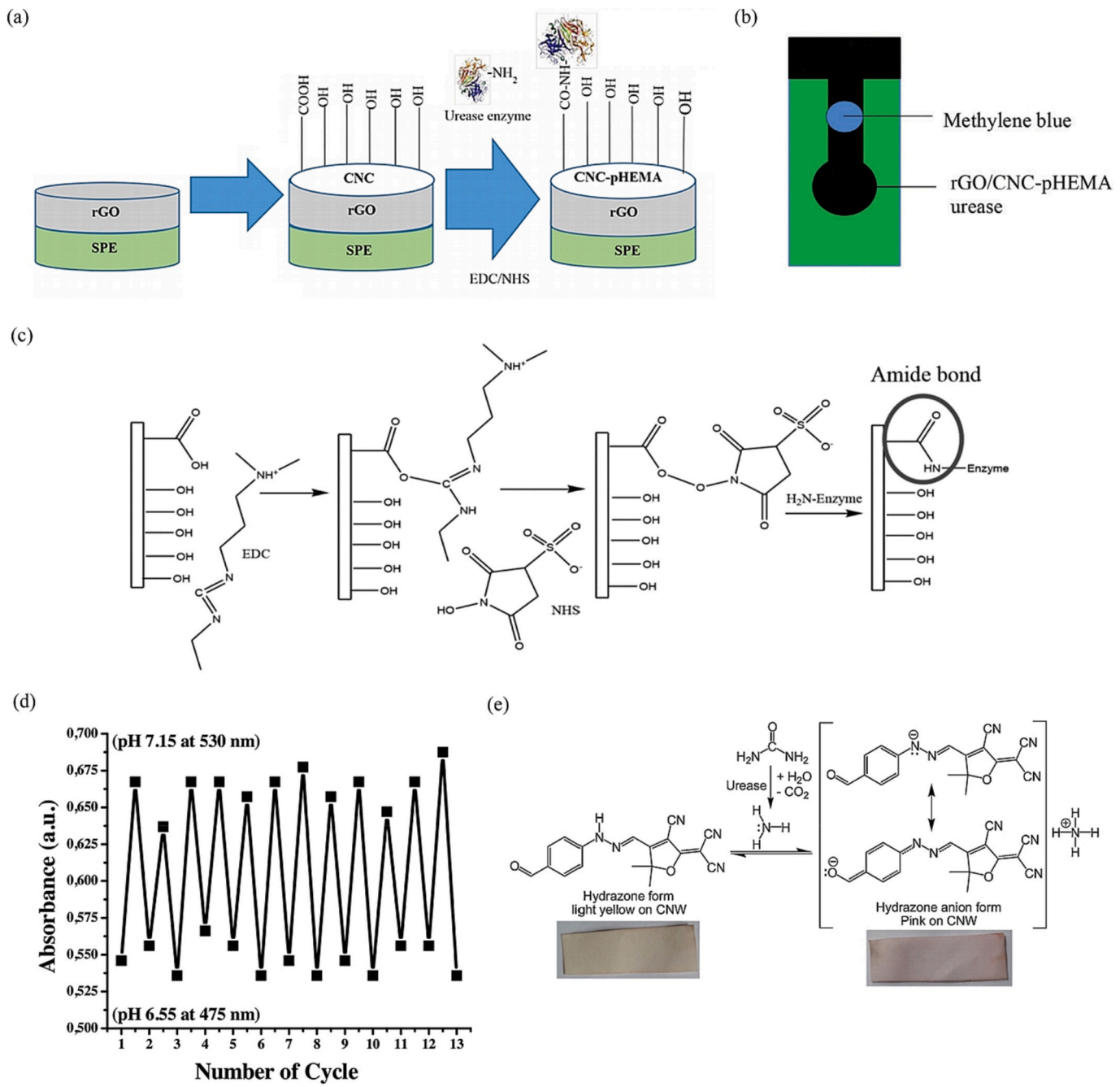


**Fig. 3.** (a) Step-by-step urea sensor fabrication; (b) the modification of rGO/TOCNC-polyHEMA-urease electrode with MB. (c) Immobilisation of urease enzyme on TOCNC in the presence of NHS and EDC (Khalid et al., 2018); (d) UV–Vis adsorption intensity in pH = 7.15 (at 530 nm) and pH = 6.55 (at 475 nm); (e) mechanism of TCFH colour alteration in exposure to urea from light yellow to pink (Khattab et al., 2020).

of urease onto high-content nanocellulose dialdehyde (HANCD) under moderate operational conditions. HANCD was prepared via acid hydrolysis and periodic oxidation from nanocellulose isolated from cotton. The resultant sensor could efficiently estimate the concentration of urea in blood serum. Another colourimetric sensor for fast urea diagnosis (5–10 min) in blood and serum was built by Khattab et al. (2020). In all studies outlined in this review for urea recognition, enzyme immobilisation was the inseparable stage of sensor development. Besides, the existence of a pH-responsive substance and sensing mechanism are somewhat similar. However, the materials used for immobilising enzymes and indicating pH are different. In the work of Khattab et al. (2020), various contents of tricyanofuran-hydrazone (TCFH), acted as a pH-responsive element, and the urease enzyme was incorporated into alginate/rice-straw-derived CNW. In the end, the attained mixture was cast on Whatman paper. The reaction between urease and urea led to the production of ammonia, an increase in pH and colour changes. The colour of TCFH in exposure to urea (in pH = 6.55–7.15) altered reversibly from light yellow to pink. It was deployed for several cycles, and the reversible colour change was fulfilled based on the push-pull molecular system, in which TCF and H acted as an acceptor and a donor, respectively (Fig. 3(d, e)). The sensing platform containing 1.5 wt % TCFH showed the most precise performance with 50–1100 $mg.L^{-1}$ detection limit. The simple preparation and favourable performance of the resulting sensor made it a decent option for monitoring urea in food and products containing urea.

#### 2.1.6. Other biomarker sensors

There are some biomarkers for which few studies have fabricated a sensor. Some of the most recent works are described in the following. Fan et al. (Fan et al., 2018) invented a biosensor detecting vitamin C in a range of 0.8–15,000.0 μmol.$L^{-1}$, as well as recognising it in the existence of UA and DA. For fabricating this biosensor, gold NPs (AuNPs), produced through the reduction of gold (III) chloride hydrate ($HAuCl_4$) with sodium borohydride ($NaBH_4$), were stabilized on the surface of C-CNC. Afterwards, the porous and conductive nanocomposite in which AuNPs/C-CNC was utilised as a dopant for the polymerisation of poly(3,4-ethylene dioxythiophene) (PEDOT) was deposited on GCE. This biosensor worked on a basis of current, which was ascribed to the concentration of vitamin C and triggered by applying the potential of −0.15 V.

Rebelo et al. (2019) modified BC with polyvinyl aniline (PVAN)/PANi bilayer to construct an electrochemical biosensor identifying neurons. This was achieved through the consecutive polymerisations of 4-vinylaniline and aniline, which were carried out via surface-initiated atom transfer radical and in-situ chemical oxidative methods, respectively. Indeed, the formation of PANi, boosting electrical conductivity, was enhanced by the PVAN interlayer. The obtained nanocomposite was sensitive to voltage alterations induced by charge-transfer redox reactions on the surface of the PVAN/PANi bilayer. This nanocomposite was able to discriminate between specialised and mature neurons in the subventricular zone via stimulation and did not have any cytotoxic effects. This work paved the way for the establishment of a novel sensor for regenerative nerve medicine, requiring non-cytotoxicity and electroconductivity.

Tabatabaee, Golmohammadi, and Ahmadi (2019) produced a disposable (nanopaper-based assay tool), reasonable (~ €0.01 per test) and user-friendly (visual detection by smartphone readout) biosensor that could determine bilirubin (BR), which is an indicator of jaundice/hyperbilirubinemia, in infants' blood. They embedded photoluminescent CD as a sensing resource in BC nanopaper which was integrated with a smartphone. The mechanism for BR sensing was on a foundation of recovering the photoluminescence, quenched in the existence of BR, upon being exposed to blue light (λ = 470 nm). This recovery happened because of the photoisomerisation and photooxidation of BR, through which unconjugated BR changed into colourless oxidation products. The results acquired from the comparison between the developed biosensor with the clinical method showed that it can be exploited for real-time jaundice diagnosis, due to its non-toxicity and superior physicochemical characteristics.

BC has been employed extensively as a substrate in biosensors, and in all the studies described above, BC was employed as a substrate. Indeed, cellulose-based substrates provide biosensors with quick adsorption of analytes into the recognition sites because of their porous structure and vast surface area (Kamel & Khattab, 2020; Li et al., 2016).

Another sensor in which BC was applied as a substrate was fabricated by Gomes, Carrilho, Machado, and Sgobbi (2020). This sensor was able to identify lactate in sweat by analysing the amperometric responses. Lactate is produced from pyruvate via anaerobic glycolysis and exists in body fluids. Lactate, a paramount glucose generator, is a determining factor for appraising some physiological processes, including sepsis, wound regeneration and muscle fatigue, which result in various diseases (Lin, Muthukumar, & Prasad, 2020). BC, with its superb mechanical resistance, made the sensor flexible and a promising candidate for wearable devices. The fabrication of the sensor was done through the modification of SPE by Prussian blue nanocubes (PBNcs)/Nafion and lactate oxidase (Lox), which were directly immobilised on BC. This non-invasive analytical device possessed a quantification limit of 4.38 mmol.$L^{-1}$ and a LOD of 1.31 mmol.$L^{-1}$.

Saylan et al. (2020) designed a sensor for detecting thymidine (Thy), a kind of nucleoside, based on the MIP technique. Nucleosides, formed via the combination of the organic base and a five-carbon sugar, have an assortment of curative applications, and their timely detection in cancer biomarkers is indispensable. In this study, the pre-complex required for imprinting was attained through the addition of N-methacryloyl-L-Cys methyl ester (MAC), an amino acid-based monomer and $Cu(NO_3)_2$ $2{\cdot}5H_2O$ to Thy as a template molecule. Afterwards, it was added to silanised magnetic BC (mBC-Si) to produce Thy-imprinted mBC (mBC-Thy). Finally, the template molecule was removed from mBC-Thy, leaving cavities that contained metal–chelating agent and MAC. These cavities were considered recognition sites for Thy nucleoside. This claim was proved by comparing the selectivity of this platform towards Thy in the mixture of two other competitive nucleosides (cytidine and uridine). The selective adsorption of Thy nucleoside was respectively 4.13 and 3.80 times higher than that of Cytidine and Uridine nucleosides at the same concentrations. This phenomenon is because of the spatial orientation of the functional groups of Thy, which fitted the spatial integrity of the cavities more. Also, the spatial arrangement of MAC and metal–chelating agents in the cavities could be another reason. Besides mBC-Thy, non-imprinted mBC was produced through a similar method in the absence of Thy, and its sensing performance was compared to mBC-Thy. The selectivity of non-imprinted mBC towards all named nucleosides was the same since no cavity was engendered.

### 2.2. Bacterial sensors

The detection of bacterial pathogens is important in medicine, food safety and public health. Bacterial infection is a major cause of diseases and mortality worldwide. These infections are often misdiagnosed, or the diagnosis process has an unacceptable delay. Current methods of bacterial identification and detection rely mainly on laboratory-based techniques, such as cell culture, biochemical kits and microscopic analysis. These methods are laborious, costly, time-consuming and require special equipment. Over the last few years, there have been great efforts to develop new biosensors for the detection of bacteria (Choi, 2020; Feng, Zhou, Gao, & He, 2020; D. Han et al., 2020). Biosensors have proved a promising technique for bacteria diagnosis and detection due to their sensitivity, portability, rapidity, selectivity and easy miniaturisation (Ahmed, Rushworth, Hirst, & Millner, 2014; Jiang et al., 2020; Riu & Giussani, 2020).

Nanocellulose-based hybrid materials have been used in biosensors to detect bacteria. As an example, the timely and precise detection of *Staphylococcus aureus* (*S. aureus*), the reason for many infectious diseases, was done by using a sensor composed of AuNPs, carbon NPs (CNPs) and CNF. This sensor was capable of recognising this bacteria in human blood serum (Ranjbar & Shahrokhian, 2018). Tuberculosis (TB) disease, usually caused by *Mycobacterium tuberculosis* (MTB), is the foremost factor in a substantial number of people's deaths. The early diagnosis of this disease prevents TB from becoming an epidemic. Recently, Zaid et al. (2020) made a novel electrochemical biosensor for MTB detection. It was produced by the dispersion of rGO in TONCC, and the $NH_2$-rGO/TONCC nanohybrid films were drop-coated on a screen-printed carbon electrode (SPCE). Eventually, the peptide nuclide acid (PNA) was immobilised on the resultant platform. Then, the hybridisation of this PNA-based biosensor was done by drop deposition of intended DNA. At last, it was immersed in MB, acting as an electrochemical indicator, to be prepared for electrochemical analysis. Fig. 4(a) displays a schematic of the described procedure. Interestingly, the hybridisation of the PNA-based biosensor was implemented by one-base mismatch, non-complimentary and complementary DNA strings of MTB, and the biosensor was able to distinguish them. As can be seen in Fig. 4 (b, c), the PNA-based biosensor was selective towards complementary DNA with a wide linearity range. This sensor can also be exploited for the immediate recognition of this bacteria in the sputum samples of humans with the polymerase chain reaction product of MTB DNA.

Later, they invented another electrochemical biosensor for the same target with higher LOD and a narrower linearity range. Fig. 4(d, e) proves this fact via comparison to Fig. 4(b, c). In Fig. 4(d), in the plot of current potential, the peak occurred at a higher level (indicative of

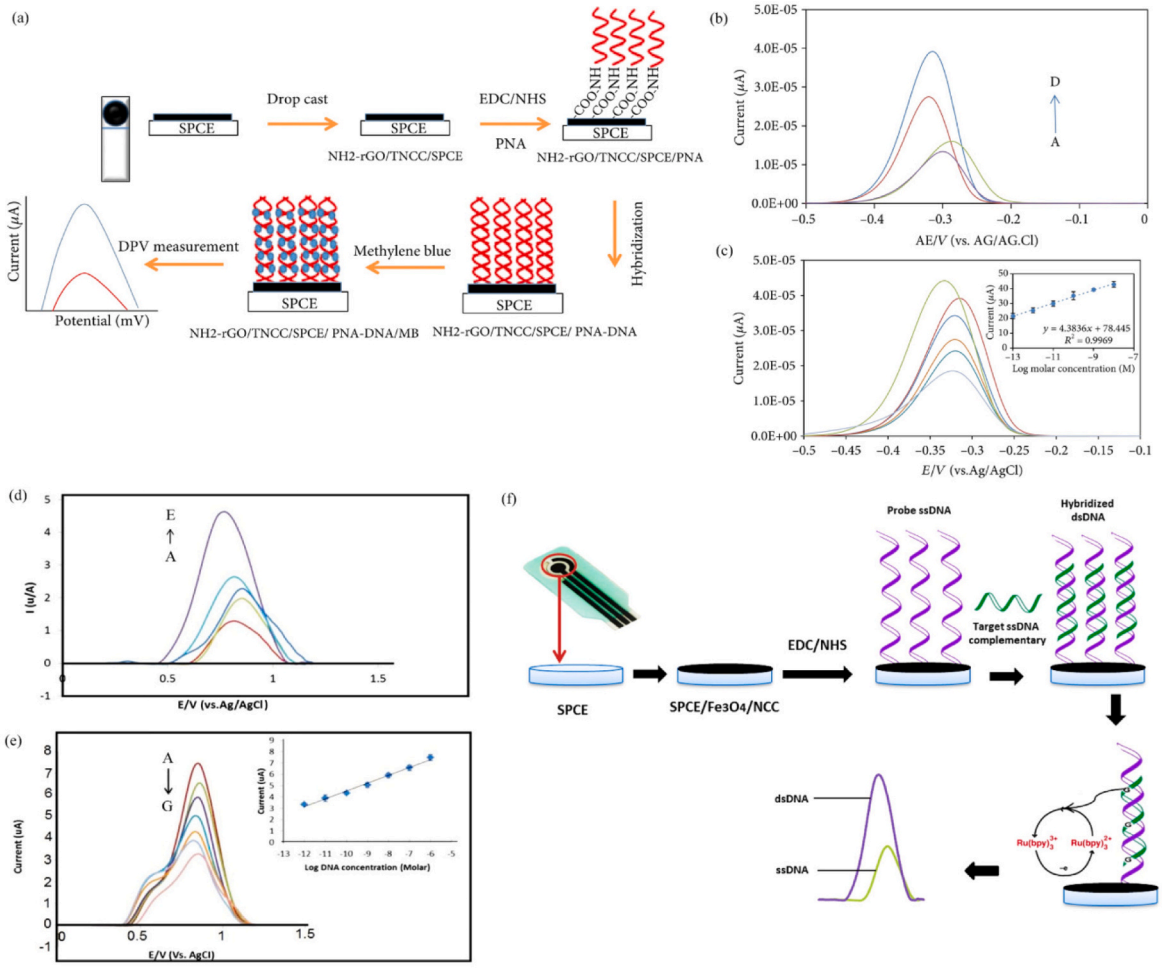


**Fig. 4.** (a) Schematic of the experimental procedure of PNA-based biosensor production and hybridisation process; (b) selectivity of PNA-based biosensors towards variant kinds of DNA: (A) PNA only, (B) non-complimentary, (C) one-base mismatch, (D) complementary; (c) linear relation of DPV peaks against the current in a $10^{-13}$–$10^{-8}$ mol.L$^{-1}$ concentration range of complementary DNA (inset: calibration plot of complementary DNA in the $10^{-13}$–$10^{-8}$ mol.L$^{-1}$ concentration range, Zaid et al., 2020); (d) DPV curve of Ru(bpy)$_3^{2+}$ oxidation for various probes: (A) lacking DNA probe, containing (B) only DNA probe, (C) mutation-DNA, (D) non-complimentary DNA, (E) complementary DNA; (E) linear relation of DPV peaks against the current in a $10^{-12}$–$10^{-6}$ mol.L$^{-1}$ concentration range of complementary DNA (inset: calibration plot of complementary DNA in the $10^{-12}$–$10^{-6}$ mol.L$^{-1}$ concentration range); (F) schematic of the experimental procedure of DNA biosensor production and hybridisation process (Zaid, Che-Engku-Chik, et al., 2020).

higher LOD) within a narrower range. To develop this biosensor, the composite of CNC and $Fe_3O_4$ was functionalised with mercaptopropionic acid (MPA) NPs and cetyl trimethyl ammonium bromide (CTAB), respectively, and cast onto SPCE. Subsequently, by using a coupling mechanism, a special string of MTB DNA, which was named the DNA probe, was immobilised on it. Following previous work, a hybridisation process was performed. In this sensor, ruthenium bipyridyl Ru(bpy)$_3^{2+}$ was utilised for better electrochemical response and signal amplification acquired from DPV measurement (Fig. 4(f)). Ru(bpy)$_3^{2+}$ and DNA with respective charges of positive and negative interacted with one another, ending in the drastic increase in DPV peak current. The fabricated biosensor detected target DNA in a wide range of concentrations from $10^{-12}$ to $10^{-6}$ mol.L$^{-1}$ (Zaid, Che-Engku-Chik, et al., 2020).

## 3. Chemical sensors

Chemical sensors are kinds of analysers providing real-time data of a chemical system composed of one or more variant chemical components (Aaryashree et al., 2021). The performance of these sensors is based on the conversion of chemical data into read-out signals, such as changes in absorbance and relative resistance, conductance and voltage. The chemical data could be the concentration of an analyte or total composition analysis (Dai, Liu, & Wei, 2022).

### 3.1. Ion/drug sensor

Any infection in the skin and gingiva or any disease in dental, renal and metabolic systems brings about pH change in human body fluids. Concerning this fact and a rapid increase in requests for healthcare, a great many researchers concentrate on tracing pH levels in body fluids (Yoon et al., 2020). A simple, reversible, quick and user-friendly colourimetric pH-responsive sensor was reported by Khattab, Dacrory, Abou-Yousef, and Kamel (2019) for onsite sweat monitoring. This sensor, which was applicable for drug testing via direct contact with skin, was generated based on embedding tricyanofuran hydrazine-sensitive dye into sponge-like MFC aerogel. Microporous MFC aerogel substrate was prepared via freeze-drying the phosphoric acid hydrolysed wood pulp. On the other hand, tricyanofuran hydrazone probes with acid-base characteristics acted as detection sites, which contributed to the determination of sweat pH range by converting from yellow to orange, red and blue as a sequel to the reversible deprotonation-protonation process. Moreover, the solvatochromic efficiency of the tricyanofuran hydrazone probe in solvents with various polarities and its pH-related colour alteration in acetonitrile were analysed utilising

UV–Vis. The sensor showed subtle cytotoxicity to the skin and did not require intricate electronic tools or a professional operator.

In recent decades, the increase in industrial activities has aroused a severe concern about health issues influenced by cations, anions and heavy metal pollution (e.g. $Fe^{3+}$, copper ($Cu^{2+}$) and manganese ($Mg^{2+}$), among others). Controlling the levels of such ions and taking part in pathological and physiological reactions has necessitated the development of chemo-sensors for identifying chemicals (He et al., 2019; Ravichandiran et al., 2020; Zhao et al., 2019). As the utilisation of conventional techniques for determining the level of heavy metal ions is time-consuming, sophisticated and needs skilful operators, the ion-selective sensors have been widely regarded as a substitution for them. Ion-selective sensors must possess analytical characteristics, such as ultra-sensitivity, selectivity, fast response and durability (Yavuz et al., 2021).

The identification of varying concentrations of ammonium ion ($NH_4^+$), as one of the utmost metabolism indicators in the human body, is a weighty matter. Kim et al. (2019) created a 3D-printed wireless $NH_4^+$ selective and sensitive sensor (3.4 % $L.mol^{-1}$, comprising inductor-capacitor circuits and ion-selective membrane electrodes. Ion concentration changes were identified using a vector network analyser based on the estimation of reflection coefficient and resonant frequency ($R_f$) intensity at 2.36 GHz. In this sensor, the conductive ink consisted of a mixture of AgNWs, CNF and CNC that was 3D printed on hydrophobic polyimide (PI) film. The fabrication was optimized by the incorporation of various weight ratios of AgNWs into CNF and CNC. Both CNF and CNC, as the main materials for additive manufacturing, could be employed as 3D printable ink substances with the shear-thinning feature. Nevertheless, 3D-printed AgNWs-CNF demonstrated far better conductivity in comparison to 3D-printed AgNWs-CNC in analogous conditions due to the random distribution of AgNWs in 3D-printed AgNWs-CNF.

$Fe^{3+}$ is an indispensable element in the human body, playing a vital role in several biochemical reactions whose deficiency causes some illnesses. However, as the overload of this element in the body affects human health adversely, so its monitoring is of great importance (Lesani et al., 2020). In recent years, the application of fluorescent probes in $Fe^{3+}$ detection has been studied. For materials without fluorescence characteristics, such as nanocellulose, several indirect fluorometric methods, like fluorescence quenching, fluorescent complex formation and derivatization can be deployed. Fluorescence quenching is the method which has been the most reported one for $Fe^{3+}$ diagnosis (Karuk Elmas et al., 2020; Li, Mei, Chang, Xu, & Yang, 2020). In this context, Chen et al. (2019) prepared a remarkably sensitive $Fe^{3+}$ fluorescent sensor that operated based on fluorescence quenching via a facile single-step method. In summary, MCC was treated with citric acid/Cys and acid hydrolysed under severe conditions. MCC hydrolysis, cellulose esterification and citrate-based fluorophore were carried out at the same time, leading to the isolation and functionalisation of CNC. The isolated CNC was 156 nm in length and 7.9 nm in width. This sensor showed favourable photostability (stable fluorescence intensity in a broad range of pH values and ionic strengths), high quantum yield (83 %) and maximum excitation and emission wavelengths at 350 and 435 nm, respectively. Furthermore, the insignificant cytotoxicity of the sensor made it a promising candidate for utilisation in $Fe^{3+}$ detection in living cells.

Another issue, which is of great significance and should be considered, is the differentiation of therapeutic drugs in body fluids. The purposes of this issue are to reduce doping in sports, make sure that patients are consuming an accurate dosage, investigate the physiological performance of drugs, diminish the dangers ascribed to drugs and curtail misuse (dos Santos, Amin, & Compton, 2019; Özbek, Berkel, & Isildak, 2020; Teymourian et al., 2020). In this regard, Faham, Golmohammadi, Ghavami, and Khayatian (2019) designed an efficient assay kit that was able to recognise not only $Fe^{3+}$ but also a kind of iron-chelating drug via a one-step method. In summary, they embedded curcumin in BC nanopaper (CEBC) for diagnosing deferoxamine (DFO), and it was applied for treating accumulated $Fe^{3+}$, besides recognising $Fe^{3+}$ in blood serum, urine and saliva. Despite the positive effects of DFO, the elevated level of this drug has several side effects. As a result, DFO determination is an essential issue in healthcare. Fig. 5(a, b) shows the scanning electron microscopy (SEM) images of BC and CEBC containing curcumin. The mechanism of $Fe^{3+}$ diagnosis was based on the reduction of the absorbance/colour intensity of CEBC through forming a $Fe^{3+}$-curcumin complex. Conversely, the DFO discrimination strategy was based on an increase in the absorbance/colour intensity of CEBC, accomplished via releasing $Fe^{3+}$ from the $Fe^{3+}$-curcumin complex because of the strong affinity of DFO with $Fe^{3+}$. Absorbance/colour intensity alterations were tracked using a smartphone and spectrophotometer (Fig. 5(c-e)).

Diclofenac sodium (DCF), a broadly taken painkiller, is prescribed for joint degenerative disease and arthritis. Nonetheless, the long-term consumption of this drug will cause people afflicted by diabetes or Shy-Drager syndrome to have strokes and heart attacks. Shalauddin et al. (2019) made an electrochemical sensor selective to DCF from ampoules, tablets, urine specimens and blood serum. The deposition of functionalised MWCNTs (f-MWCNTs) on nanocellulose was conducted on GCE and its selectivity and sensitivity were determined using DPV and CV techniques. At optimum conditions, the peak current rose substantially (41.6 μA) for 50 $\mu mol.L^{-1}$ DCF at 0.677 V peak potential. In this sensor, hydroxyl groups existing in the nanocellulose not only acted as hosts for various analytes but also enabled an axial modulus array and the integration of f-MWCNTs. On the other hand, f-MWCNTs boosted electrical conductivity, mechanical properties and surface area, resulting in improving the electrochemical sensing of DCF.

As a drug for treating neurological disorders, olanzapine (OLZ) was identified with a highly selective electrochemical sensor designed by Mahmoud et al. (2020) and used in real specimens. The nanohybrid was produced by merging nanocellulose and nitrogen, sulphur co-doped GQDs (N, S@GQDs) together, followed by casting on GCE. The modified GCE accomplished proper OLZ adsorption and oxidation due to the synergistic effect of nanocellulose and N, S@GQDs. Additionally, it had a vast linear range and a low amount of LOD.

Venlafaxine is a kind of antidepressant medicine that is often used to treat major depressive disorders. It has curative properties for patients suffering from depression, panic disorders and anxiety by augmenting the amounts of natural ingredients in their brains and bodies. Khalilzadeh, Tajik, Beitollahi, and Venditti (2020) constructed an accurate, low-price, stable, selective and easy-to-use electrochemical sensor for venlafaxine diagnosis in urine and other pharmaceutical formulation specimens. In this context, graphite SPE (GSPE) was modified with magnetic $Fe_3O_4$@CNC/Cu nanocomposite. The formation of this nanocomposite was proved by using spectroscopic, microscopic, magnetometer and diffraction analyses. The modified GSPE displayed satisfactory electro-catalytic behaviour towards venlafaxine. In this sensing platform, CNC, extracted from *Petasites hybridus* leaf via the green method, acted as a stabilising and reducing agent for Cu.

Among chemo-sensors lately invented based on nanocellulose for clinical applications, there is a sensor for detecting methylparaben (MP), thereby considered an organic chemical compound. MP, with negligible toxicity, is a type of preservative in cosmetics and healthcare products. Faradillawan Khalid et al. (2019) drop-cast the nanocomposite of CNC-rGO on SPE to develop this sensor, demonstrating competent stability, repeatability and reproducibility (RSD = 8.2 %).

## 4. Physical sensors

Physical sensors can detect physical stimulus changes and convert them into electrical signals. Such sensors are categorised into strain, pressure, temperature and humidity sensors and play crucial roles in human health monitoring, medical healthcare and so forth. Human activities, which engender physical stimuli, including heartbeat, blood pressure, foot pressure, skin surface temperature and skin strain, can be

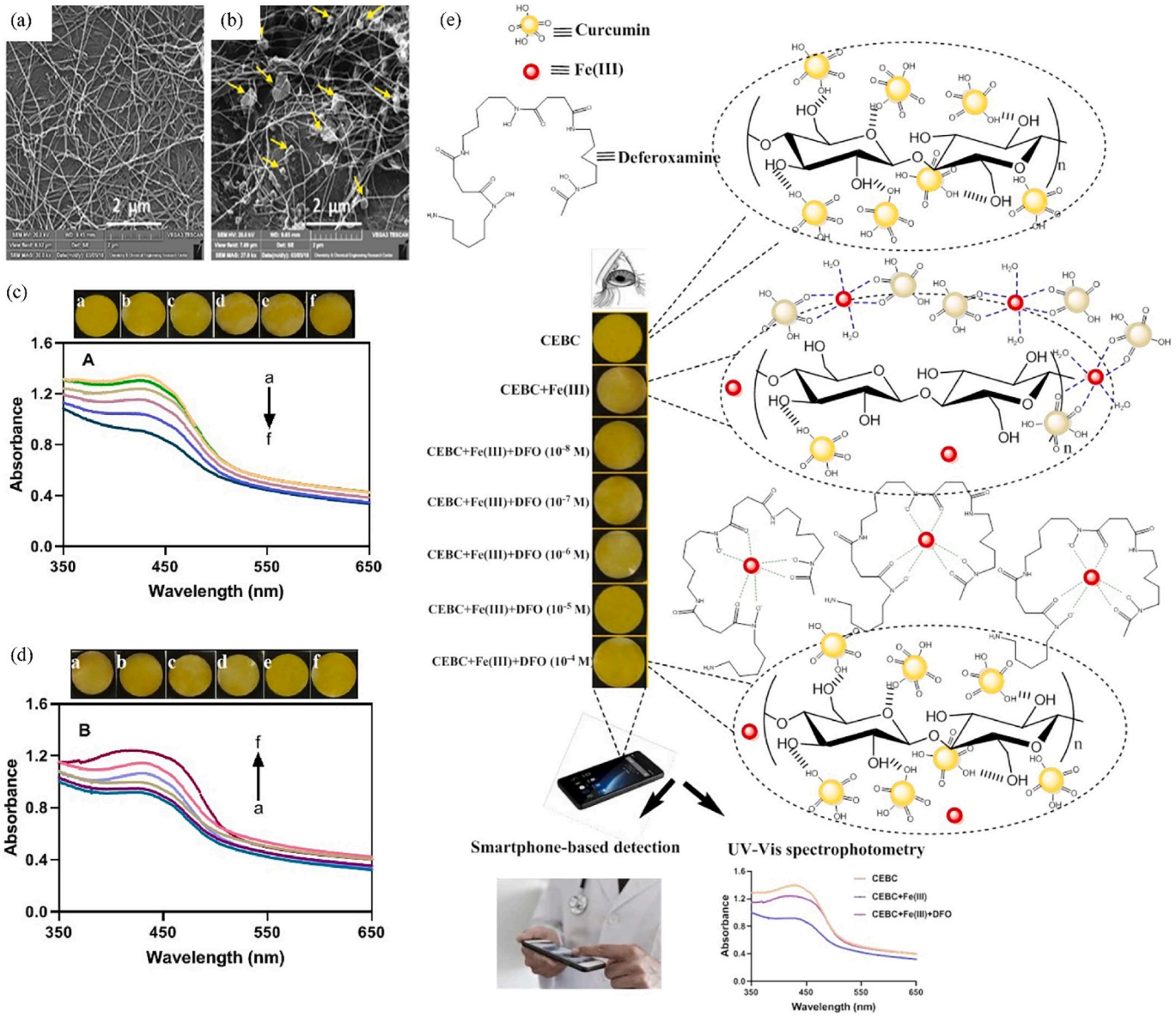


**Fig. 5.** SEM images of (a) BC nanopaper and (b) CEBC. UV–Vis absorption spectra of (c) CEBCs in the existence of variant $Fe^{3+}$ concentrations and (d) CEBC-$Fe^{3+}$ in the existence of variant DFO concentrations alongside the relevant photos; (e) mechanism of $Fe^{3+}$ and DFO diagnosis using smartphone and spectrophotometer (Faham et al., 2019).

considered health indicators and be monitored by physical sensors (Huang, Zhao, Hao, & Wei, 2022). Regarding this, numerous studies have been done to develop these kinds of sensors for tracking such health indicators. Some of these studies are outlined in the following.

### 4.1. Pressure/strain sensors

The stretchable strain sensors, commonly include piezoresistive, piezoelectric and capacitive sensors, consist of electrodes and sensing components which are the primary parts for identifying changes in signals (Chen & Yan, 2020). Because it is renewable, dispersible in water and shows favourable mechanical behaviour, nanocellulose has drawn great attention to be used in strain sensors. However, it does not demonstrate the sensing ability for recognising mechanical stimuli (Yan, Zhou, & Fu, 2020). In this case, conductive materials are considered efficient substances in manufacturing ingenious structures for enhancing the performance of strain sensors (Chen et al., 2020; Zheng et al., 2020). Such materials are mostly integrated with nanocellulose via carbonisation, mixing and coating and are fabricated in different forms, such as films, papers, fabrics, fibres and gels (Chen, Yan, & Pan, 2021). Among other applications, the employment of conductive hydrogels in wearable and flexible sensors has recently gained considerable attention, and several researchers have focused on this type of biosensor.

Tannic acid (TA), as a kind of plant polyphenol, possesses five groups of each pyrogallol and catechol. It has been recently utilised to prepare hydrophilic coatings. Catechol/pyrogallol groups adhere to the substrate utilising hydrogen bonds, electrostatic or hydrophobic interactions and covalent reactions to create mussel-inspired hydrogels (Fang et al., 2020; Nath, Saikia, Handique, Gupta, & Dolui, 2020). To exemplify, Lu et al. (2020) invented a conductive hydrogel sensor that was able to track the human wrist and finger. This sensor was fabricated by coating TA on the CNF surface to construct a hydrogen skeleton, subsequently combined with poly(acrylamide) (PAAM) and $Fe^{3+}$ by metal coordination. $Fe^{3+}$, as an inorganic conductive phase that was chelated via metal coordination, conferred favourable electrical

conductivity (up to 3.12 $S.m^{-1}$). Besides, the obtained sensor indicated substantial mechanical properties (storage modulus of >14 KPa and fracture stress up to 108 KPa). Here, nanocellulose was applied to build a self-adhesive, robust and tough conductive hydrogel through physical interactions and erecting a synergistic cross-link network.

Another strain sensor mimicking the adhesion of mussels was developed by Yan et al. (2020). Firstly, CNC isolated from bamboo pulp via acid hydrolysis was coated with PANi (PANi@CNC). Secondly, the product of the previous step was dissolved in TA. Finally, the TA/PANi@CNC platform was immersed in an $AlCl_3$ aqueous solution for metal-phenolic network formation. The obtained nanocomposite hydrogel demonstrated superior stretchability (974 %) and breaking strength (759 KPa), self-healing (within 30 min) and self-adhesion (no need for extra fixation on the skin), as well as outstanding electrical conductivity (resistivity of 0.5 Ωm). It was able to track even pulse and water droplets, culminating in being a promising device for human healthcare and motion tracing. In this sensor, CNCs played a significant role in improving fracture strength because of their hydrogen interactions.

Song et al. (2020) produced a strain sensor in which multi-branched CNC (Multi CNC) was deployed as a template that prevented PANi from aggregation besides serving as a dynamic bridge and hydrogen bonding. The final sensor, which was manufactured through the combination of Multi CNC-PANi with polyvinyl alcohol (PVA) and borax, hydrogen and dynamic borax bonds, as well as hierarchical CNC, improved its self-healing feature. It could get self-healed up to 99.56 % in 2 min. This sensor indicated 171.52 KPa breaking strength and 1085 % stretchability. Zhang et al. (2022) designed another self-healing hydrogel based on PVA, borax and CNF which was able to detect the minimum weight of 5 g. This system could recover its initial form within 5 min and maintain its sensitivity in a range of 0–60 °C. In another investigation, Chen, Zhu, Yu, and Li (2020) fabricated a conductive self-healable composite film containing CNC-polypyrrole (PPy) in combination with PVA and methyl methacrylate (MMA). This composite film with soft-hard architecture exhibited considerable electrochemical properties and sensitivity to body movements. For the fabrication of this sensor, PPy was prepared via in-situ oxidative polymerisation and coated on CNC. Then, the one-pot method was carried out for the polymerisation of MMA (hard segment) on the functionalised CNC and the process continued with mixing the attained nano-network with PVA (soft segment). The addition of 2 wt% CNC-PPy enhanced the tensile strength of the composite film by 47.1 %. CNC as a biomass template facilitated the PPy ideal dispersion culminating in the formation of a reinforced network with conductive properties in the PMMA/PVA matrix because of the hydrogen bond dynamic network. Zhuo et al. (2019) designed a 3D piezoresistive hydrogel that operated as a wearable strain sensor with wonderful mechanical performance. They used CNC as a nano-support for the connection of MXenes sheets to lamellar carbon with a wave-shaped structure. This sensor possessed a 114.6 $kPa^{-1}$ sensitivity and a 1.0 Pa LOD, so it was able to detect the pressure created by 10 μL of water. Additionally, it withstood 95 % compression strain as well as prolonged compression (10,000 cycles at 50 % strain).

Wu et al. (2020) designed another conductive hydrogel that could be applied for the fabrication of highly efficient electrical conductive tools, such as stretchable sensors and supercapacitor electrodes. This composite hydrogel was able to trace motions in the forehead and the joints of the knee, elbow and finger. In addition, it could rapidly respond to pressing and cyclic tensile forces. It also possessed great electrochemical properties, namely 60 % capacitance retention and ~ 65 $F.g^{-1}$ specific capacitance after 2000 cycles. In this work, TONC was used for stabilising CNT into a pigskin (PS) matrix. Indeed, Chinese cuisine was exploited as an inspiration for designing this sensor. In all these outlined research studies, the coating method was employed for the integration of conductive materials on nanocellulose. Another study conducted by Zheng et al. (2020), was allocated to the fabrication of a conductive hydrogel, as a highly sensitive strain sensor, via mixing the conductive materials with nanocellulose (Fig. 6(a)).

This hydrogel was prepared through the dispersion of TOCNF-graphene (GN) composite in polyacrylic acid (PAA), formed via in-situ free radical polymerisation. The preparation process and the formation mechanism of the hydrogel are illustrated in Fig. 6(b, c). The fabricated wearable sensor exhibited excellent mechanical properties and healing ability and was able to monitor finger, arm and leg bending. As depicted in Fig. 6(d, e), the responses of the sensor to writing various alphabets (N, J, F, U) were different from one another. Furthermore, Fig. 6(f, g) demonstrated that the obtained sensor, attached to the arm and leg, could distinguish between bending and releasing based on the output current. The aforementioned properties showed that the designed sensor would have a substantial potential for different applications in an assortment of fields, including electronic skins and robotics, among others.

In a work carried out by Su et al. (2022) a dual-network hydrogel was developed with the inspiration from animal muscle via the integration of GO@nanocellulose into a poly(AAm-*co*-AAc) network. This phenomenon raised the average elongation at the break of the nanocellulose network from 86.2 % to 748.0 %. Furthermore, the rupture tensile strength of poly(AAm-*co*-AAc) rose by 228.6 %. The obtained platform was able to retrieve 85 % of its initial shape after 600 s.

### 4.2. Temperature sensor

Thermo-responsive hydrogels have attracted a great deal of attention in biomedical applications, such as implants, drug delivery and wound healing owing to their unique mechanical performance (Talantikite et al., 2021). Conventional temperature sensors work on a foundation of heat flow by utilising invasive probes, having pretty low precision and being affected by interfering signals which cause measurement errors. In this case, the demand for the construction of novel temperature sensors has increased (Zhang et al., 2019).

Talantikite et al. (2021) prepared bio-inspired hydrogel, which comprised xyloglucan (XG) and CNC. Thermo-responsive properties and reversible thermal transition were achieved by degalactosylation of tamarind seed XG (DG-XG). The obtained results showed a reversible thermal transition for DG-XG/CNC hydrogels at 35 °C. The obtained hydrogel was devoid of hazardous components and indicated tuneable mechanical properties, which could be adjusted by changing the CNC content. In detail, different concentrations of CNC were added to DG-XG, leading to the range of CNC to DG-XG mass ratios from 300:1 to 1:20. The results attained from phase diagrams for all the samples with various mass ratios indicated that they were in a different phase, namely a thermo-responsive gel, a simple gel, a phase-separated mixture and a viscous liquid. Gelation happened at the mass ratio, which was more than the required amount for the full coverage of CNC and high concentrations of both XG and CNC (20 and 30 $g.L^{-1}$, respectively) because XG-CNC formation resulted in boosting the hydrodynamic volume of CNC. The marvellous properties of this hydrogel made it an appropriate choice for clinical applications. Another CNC-based temperature sensor was developed by Kim, Park, et al. (2019) by depositing gold nanosheet (AuNS) on PVA/CNC composite film, using the pattern transfer technique. Regarding the outcomes from 5 and 100 consecutive healing cycles and folding, respectively, this sensing device benefited from self-healing properties and stability. The optimum self-healing efficiency was gained by altering CNC contents (10 wt%), spraying solution pH (pH = 7) and temperature ($T = 45$ °C). The performance of PVA as a self-healable material, induced by the formation of dynamic intermolecular bonds and chain mobility, was improved by adding CNC as a nanofiller. However, the excessive amounts of CNC led to CNC aggregate formation and a decrease in mechanical strength.

### 4.3. Humidity sensor

The identification and tracking of water vapour in the air, which

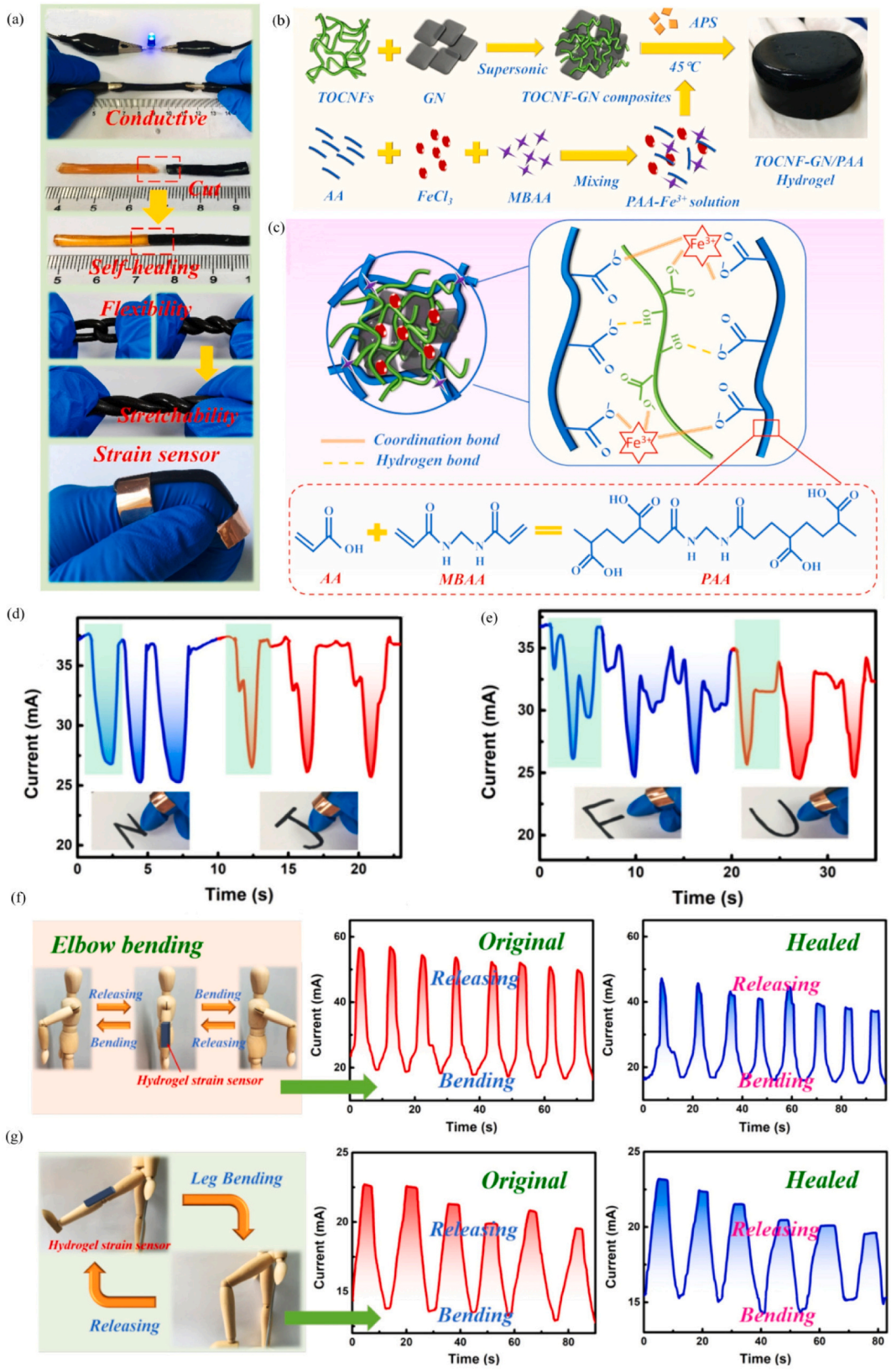


**Fig. 6.** (a) Demonstration of the conductivity, self-healing performance, flexibility and stretchability of composite hydrogel; schematic of (b) preparation process and (c) formation mechanism of the TOCNF-GN/PAA composite hydrogels; the current alterations in the sensor are triggered by writing the letters (d) "N, J" and (e) "F, U"; self-healing performance of the sensor attached to a puppet; current alterations in the sensor induced by the original and the healed hydrogels' motions in bending the (f) arm and (g) leg (Zheng et al., 2020).

affects the properties of materials drastically, is of foremost importance. Therefore, several humidity sensors were devised for various applications, such as monitoring living systems (Wang et al., 2020). CNF is considered a sensitive material towards humidity and is a promising candidate for self-standing film establishment owing to abundant hydroxyl groups on its surface. On the other hand, CNT with its hollow structure and considerable aspect ratio have striking thermal, mechanical and electrical characteristics. These features have made it an ideal component for fabricating humidity sensors (Syrový et al., 2019; Zhu et al., 2019). In this context, Zhu et al. (2019) fabricated a flexible, durable and strikingly sensitive humidity sensor based on TONFC (0.1 wt%) and different contents of CNT via vacuum filtration. The TONFC/CNT sensor containing 5 wt% CNT indicated the maximum response of 69.9 % ($\Delta I/I_0$) at 95 % relative humidity (RH). In addition, it exhibited a response in the range of 11–95 % RH, making it a great candidate for different applications in the realm of estimating humidity. The unsatisfactory flexibility of conventional inorganic sensors limits their application in the wearable electronics field.

In another study, Zhu et al. (2020) used a feasible method for the fabrication of a paper-based sensor by roll-to-roll structure to overcome this drawback. They designed a bi-layered structure sensor based on NFC/CNT and a micro-porous paper as a substrate. This foldable sensor with high sensitivity demonstrated a response of 65.0 % ($\Delta I/I_0$) at 95 % RH. This sensor, with 15 d stability, was able to tolerate 22.2 $cm^{-1}$ curvature and 50 times folding, showing that they accomplished raising the mechanical properties of their last sensor without a significant decrease in its sensitivity. It is worth noting that the obtained humidity sensors in both studies were capable of tracing human respiration.

Later, Zhu, Kuang, et al. (2021) constructed another humidity sensor based on the adsorption of positively charged CNT on TOCNF with negative charges. The positive charge of CNT was due to the existence of cationic CTAB micelles on the CNT surface, produced after the dispersion of CNC in CTAB (Fig. 7(a)). Swelling in the structure of TOCNF destroyed the conductive CNT network, promoting its sensitivity towards humidity (Fig. 7(b)). The outstanding enhancement of this sensor was in terms of its stability (over three months) and maximum response (87 % ($\Delta I/I_0$)) relative to their last two sensors; otherwise, its other properties remained constant (50 times folding durability) or decreased (2.1 $cm^{-1}$ curvature). This sensor was able to respond to fingertip and air humidity besides responding to human breath (Fig. 7(c-e)).

CNC, like CNF, is an appropriate biomaterial for developing sensing platforms owing to its great hydrophilicity, capacity for functionalisation, non-cytotoxicity and high Young's modulus. Hence, the combination of QC microbalance (QCM) with this material provides an option for building a stable and sensitive humidity sensor (Yao et al., 2020). Tang et al. (2021) devised a QCM-based humidity sensor by depositing nitro-modified CNC (NCNC) on a QCM resonator. In this study, various amounts of NCNC (0.1–0.5 $\mu g.\mu l^{-1}$) were deposited on QCM to investigate the effect of NCNC content, as a sensing film, on the sensitivity of the sensor and the obtained films were designated as QCM-x (x = 1–5). The surface of all these films was smooth because of their root-mean-square roughness. Finally, the sensor containing 2.67 μg NCNC, QCM-4, demonstrated the optimum performance with an acceptable sensitivity (25.6 $Hz.\%RH^{-1}$), fast response and recovery (18 and 10 s, respectively) at 84 % RH.

The summary of different nanocellulose-based sensing platforms developed for medical applications is listed in Table 1.

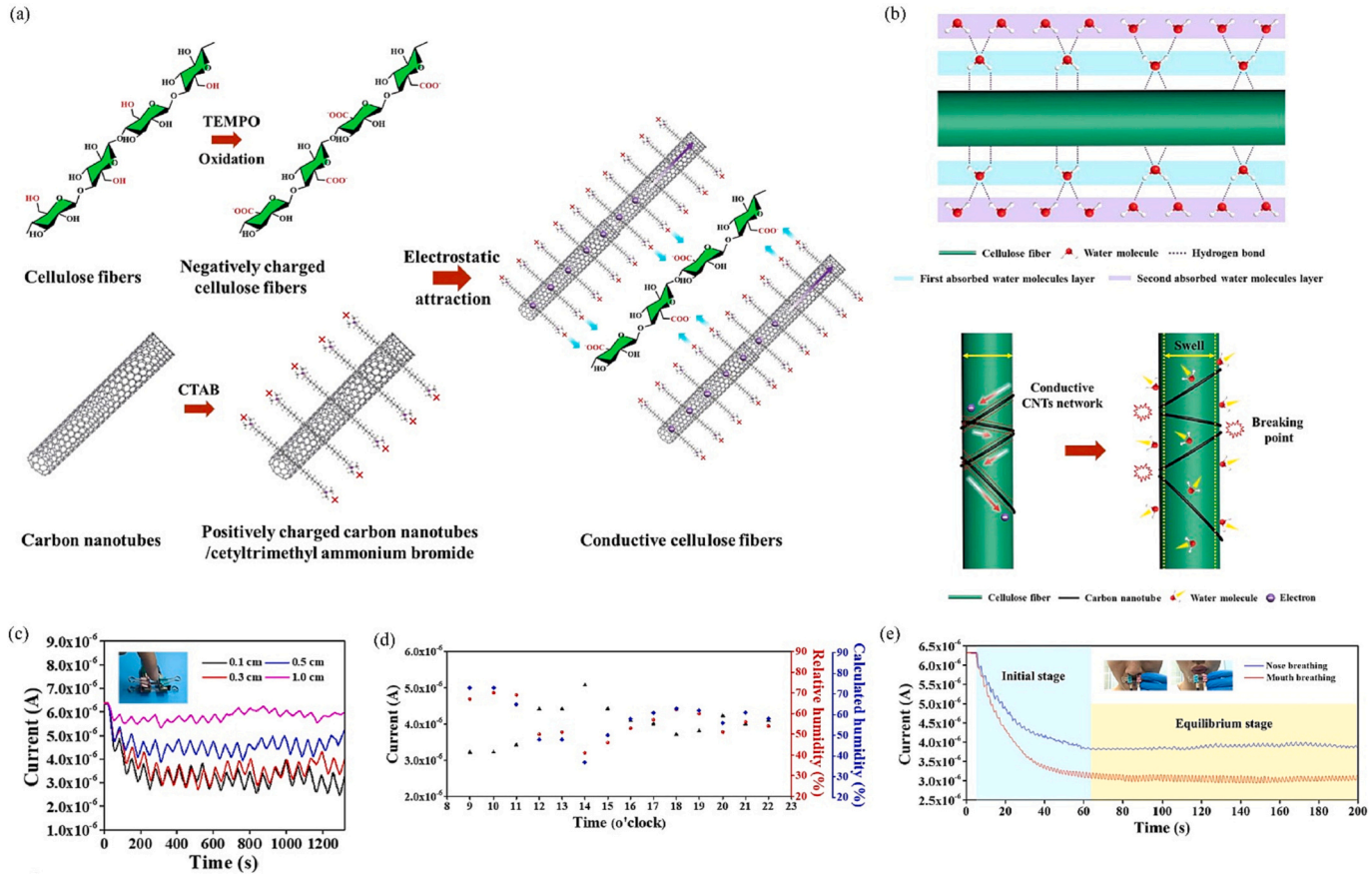


**Fig. 7.** Schematic of (a) the steps of TOCNF/CNT nanocomposite film formation and (b) the water molecule adsorption on TOCNF and the CNT network destruction, induced by TOCNF swelling; current-time plot of (c) the humidity around the fingertip for various distances (0.1, 0.3, 0.5 and 1.0 cm), (d) the air humidity during a day and (e) the human nose and mouth breathing at 33.6 and 36.8 °C, respectively (Zhu, Kuang, et al., 2021).

**Table 1**
Summary of various nanocellulose-based sensing platforms for medical application.

| Sensor category | Sensing platform | Sensing target | NC type | NC Role | Sensing source | Response range/ limit | Ref. |
|---|---|---|---|---|---|---|---|
| Biosensor | CNF-PANi-CD/SMD | Glucose | CNF | Matrix | PANi and CDs | 0.8 μmol.$L^{-1}$ | (Saikia & Karak, 2020) |
| | x-CNC-$Fe_3O_4$ | Glucose | CNC | Matrix | GOx | 5 mmol.$L^{-1}$ | (Tracey et al., 2020) |
| | C-NC/cellulose paper substrate/adsorbed GOx | Glucose | CNC | Binder | GOx | 1.5–19.0 mmol.$L^{-1}$ | (Neubauerova et al., 2020) |
| | C-NC/cellulose paper substrate/covalently binded GOx | | | | | 1.5–12.8 mmol.$L^{-1}$ | |
| | TOCNC/GOx/SPE | Glucose | CNC | Matrix/ stabilising agent | GOx | 0.1–2.0 mmol.$L^{-1}$/ 0.004 mmol.$L^{-1}$ | (Tang et al., 2020) |
| | GCE/Si-GO-g-((NC-ZnO-g-allyle amin)-IA) | Cholesterol | CNF | Substrate | GO | 5.18–25.90 μmol.$L^{-1}$/ 7.4 μmol.$L^{-1}$ | (Anirudhan et al., 2018) |
| | PANi/CNC/IL/GLU/ChOx-modified electrode | Cholesterol | CNC | Matrix | PANi and IL | 0.6475–10.3600 mmol. $L^{-1}$/ 0.0986 mmol.$L^{-1}$ | (Abdi et al., 2019) |
| | BC/GQDs-RhB | Amino acids | BC | Substrate | QD | 0.001–12.000 mmol.$L^{-1}$ /0.48 μmol.$L^{-1}$ | (Abbasi-Moayed, Golmohammadi, Bigdeli, & Hormozi-Nezhad, 2018) |
| | BC/RQDs-CDs | | | | | 8 μmol.$L^{-1}$ | |
| | s-CNC/MWCNT/GCE | Trp enantiomers | CNC | Sensing component | CNC | 0.04–4.00 mmol.$L^{-1}$/ 2.8 μmol.$L^{-1}$ | (Zhang et al., 2018) |
| | h-CNC/MWCNT/GCE | | | | | 0.04–4.00 mmol.$L^{-1}$/ 3.7 μmol.$L^{-1}$ | |
| | CNF-AgNPs | L-Cys | CNF | Reducing/ stabilising agent | AgNPs | 49 nmol.$L^{-1}$ | (Yu et al., 2020) |
| | CNF/QC substrate | Gly | CNF | Sensing film | CNF | 6–500 mg.$L^{-1}$/ 8 mg.$L^{-1}$ | (Hosseini et al., 2020) |
| | MWCNT/SNFC/Nafion/ta-C electrode | DA | NFC | Dispersant | MWCNT | 0.05–100.00 μmol.$L^{-1}$/ 65 nmol.$L^{-1}$ | (Durairaj et al., 2019) |
| | PDMS/CNC/CNT/poly (GMA-*co*-EGDMA) | Cortisol | CNC | Binder | poly(GMA-co-EGDMA) | 10–66 mg.$L^{-1}$/ 2 ± 0.4 mg.$L^{-1}$ | (Mugo & Alberkant, 2020) |
| | SPE/rGO/TOCNC-polyHEMA-urease/MB | Urea | CNC | Matrix | Urease | 0.001–0.100 mmol.$L^{-1}$ | (Khalid et al., 2018) |
| | HANCD@urease | | CNC | Stabilizer | | N.D. | (Tamaddon & Arab, 2019) |
| | Alginate/CNW/urease/ TCFH/Whatman paper substrate | | CNW | Nanofiller | | 50–1100 mg.$L^{-1}$ | (Khattab et al., 2020) |
| | PEDOT/AuNPs/C-NCC/ GCE | Vitamin C | CNC | Stabilizer | AuNPs | 0.8–15,000.0 μmol.$L^{-1}$/ 0.29 μmol.$L^{-1}$ | (Fan et al., 2018) |
| | BC/PVAN/PANI | Neuron | BC | Substrate | PVAN/PANi | N. D. | (Rebelo et al., 2019) |
| | BC/CD | BR | BC | Substrate | CD | 2–20 mg.$dl^{-1}$/0.19 mg. $dl^{-1}$ | (Tabatabaee et al., 2019) |
| | BC/PBNCs/Nafion/LOx/ SPE | Lactate | BC | Substrate | LOx | 1–24 mmol.$L^{-1}$/ 1.31 mmol.$L^{-1}$ | (Gomes et al., 2020) |
| | mBC-Si-MAC-Cu(II) | Thy | BC | Matrix | MAC, Cu (II) | N. D. | (Saylan et al., 2020) |
| | AuNPs/CNPs/CNF/GCE | *S. aureus* | CNF | Dispersant | AuNPs | 1.2–1.2 × $10^8$ cfu.$ml^{-1}$/ 1 cfu.$ml^{-1}$ | (Ranjbar & Shahrokhian, 2018) |
| | $NH_2$-rGO/TNCC/PNA/ SPCE | DNA-related TB | CNC | Matrix/ dispersant | PNA | $10^{-13}$ -$10^{-8}$ nmol.$L^{-1}$/ 3.14 × $10^{-14}$ mol.$L^{-1}$ | (Zaid et al., 2020) |
| | SPCE/MPA-$Fe_3O_4$/NCC/ CTAB/DNA | | CNC | Matrix/ dispersant | DNA | $10^{-12}$ -$10^{-6}$ nmol.$L^{-1}$/ 7.96 × $10^{-13}$ mol.$L^{-1}$ | (Zaid, Che-Engku-Chik, et al., 2020) |
| | MFC/tricyanofuran hydrazone | pH | MFC | Substrate | Tricyanofuran hydrazone | N.D. | (Khattab et al., 2019) |
| | PI/CNF-AgNWs | $NH_4^+$ | CNF | Matrix | AgNWs | N.D. | (Kim et al., 2019) |
| | CF-CNC | $Fe^{3+}$ | CNC | Matrix | Citric acid/ Cys | N.D. | (Chen et al., 2019) |
| Chemical sensor | Curcumin/BC nanopaper | $Fe^{3+}$ DFO | BC | Substrate | Curcumin | 0.01–100 μmol.$L^{-1}$/ 7.1 nmol.$L^{-1}$ 0.01–100.00 μmol.$L^{-1}$/ 8 nmol.$L^{-1}$ | (Faham et al., 2019) |
| | f-MCNTs/NC/GCE | DCF | CNC | Substrate | NC and f-MCNTs | 0.05–250.00 μmol.$L^{-1}$/ 0.012 μmol.$L^{-1}$ | (Shalauddin et al., 2019) |
| | NC/N, S@GQDs/GCE | OLZ | N.D. | Matrix | NC and N, S@GQDs | 15–900 nmol.$L^{-1}$/ 5 nmol.$L^{-1}$ | (Mahmoud et al., 2020) |
| | Fe3O4@CNC/Cu/ GSPE | Venlafaxine | CNC | Reducing/ stabilising agent | $Fe_3O_4$ and CuNPs | 0.05–600.00 μmol.$L^{-1}$/ 0.01 μmol.$L^{-1}$ | (Khalilzadeh et al., 2020) |
| | CNC-rGO/SPE | MP | CNC | Matrix | rGO | 0.2–0.9 mmol.$L^{-1}$/ 0.1 mmol.$L^{-1}$ | (Faradillawan Khalid, Nasir Mat Arip, Jasmani, & Heng Lee, 2019) |
| Physical sensor | PAAM/$Fe^{3+}$-TA@CNFs | Strain | CNF | Substrate | $Fe^{3+}$ | N.D. | (Lu et al., 2020) |
| | TA/PANi@CNC | | CNC | Substrate | PANi and aluminum ions | N.D. | (Yan et al., 2020) |
| | CNC-PANi/PVA/borax | | CNC | Template | PANi | N.D. | (Song et al., 2020) |
| | CNF/PVA/borax | | CNF | Matrix | borax | 5 g | (Zhang et al., 2022) |
| | CNC-PPy/PMMA/PVA | | CNC | Template | PPy | N.D. | (Chen, Zhu, Yu, and Li, 2020) |

(*continued on next page*)

**Table 1** (*continued*)

| Sensor category | Sensing platform | Sensing target | NC type | NC Role | Sensing source | Response range/ limit | Ref. |
|---|---|---|---|---|---|---|---|
| | C-MX/CNC | Pressure/ strain | CNC | Dispersant | MXenes | 50 Pa-10 kPa/ 1 Pa | (Zhuo et al., 2019) |
| | TONC-CNT-PS | Strain | CNC | Stabilisers, Nanofiller | CNT | N.D. | (Wu et al., 2020) |
| | TOCNF-GN/PAA | | CNF | Template/ Dispersant, Nanofiller | GN | N.D. | (Zheng et al., 2020) |
| | GO@CNC-poly(AAm-co-AAc) | | CNC | Matrix | GO | N.D. | (Su et al., 2022) |
| | DG-XG/CNC | Temperature | CNC | Adsorbent | DG-XG | 35 °C | (Talantikite et al., 2021) |
| | AuNS/PVA/CNC | | CNC | Nanofiller | AuNS | N.D. | (Kim, Park, et al., 2019) |
| | TONFC/CNT | Humidity | NFC | Dispersant | NFC/CNT | 11–95 % RH | (Zhu et al., 2019) |
| | CNF/CNT/paper | | CNF | Dispersant | CNF/CNT | N.D. | (Zhu et al., 2020) |
| | TOCNF/CNT | | CNF | Dispersant | TOCNF/CNT | 11–95 % RH | (Zhu, Kuang, et al., 2021) |
| | NCNC/QCM | | CNC | Sensing film | NCNC/QCM | 11–84 % RH | (Tang et al., 2021) |

SMD: sorbitol-based hyperbranched epoxy.
N. D.: not described.
DG-XG: degalactosylated XG.

## 5. Conclusions

In recent years, the utilisation of nanocellulose has had remarkable investigation as an innovative and efficient approach for fabricating low-price and renewable platforms for analytical devices with sensing applications in the field of medical science. Although the price of nanocellulose is higher than cellulose (0.3–0.6 cent per $m^2$) because of some extra production steps and the consumption of more energy and materials, it has been able to overcome the limitations of sensors made with cellulose-based substrates (e.g. low stability, high surface roughness and optical opaqueness). Besides, it shows low density, a larger interfacial area and a high aspect ratio (Abbasi-Moayed, Golmohammadi, & Hormozi-Nezhad, 2018). On the other hand, the price of this nanomaterial (~ $25 per kg) is less than CNTs (~ $124,000 per kg) and other synthetic nanofillers (e.g. silica particles, ceramic NPs and layered silicates) leading to more cost-effective products (Nagarajan et al., 2021). According to IUPAC, biosensors along with chemical and physical sensors are the categories considered for aforementioned devices, which could be established in different sorts of 1-dimensional (1D) (e.g. nanofibers), 2D (e.g. thin films, papers or membranes) and 3D (e.g. hydrogel, aerogel or sponges) formats. NFC, CNC and BC are different types of nanocellulose, operating as templates, nanofillers, dispersants and substrates as well as reducing/or stabilising agents in such instruments. Indeed, the existence of a great many hydroxyl groups on the surface of nanocellulose and its fibrous matrix features have made this biopolymer an option for the immobilisation of fluorescent molecules, conductive materials, plasmonic NPs, carbon-based and photoluminescent (nano)materials acting as sensing resources. The stability of such sensing elements enhances the performance of the sensors. It is also noteworthy to mention that the porous structure of nanocellulose provides an extensive surface area for this biopolymer ending in attracting more analytes.

Overall, the development of nanocellulose-based sensing composites will revolutionise state-of-the-art of medical science and disease diagnosis due to all the aforementioned advantages of nanocellulose. So far, there has been considerable progress in adding novel functionalities to nanocellulose as well as boosting its properties for fabricating sensors. However, there are still some challenges that should be addressed. As a case in point, nanocellulose is incompatible with systems containing hydrophobic polymers. Therefore, to improve their dispersion and interfacial adhesion properties, functionalised nanocellulose, coupling agents or surfactants are needed, which is not economical on a large scale. What is more, its humidity sensitivity is the main obstacle for some nanocellulose-based sensing applications as well. Importantly, despite the extensive investigation for increasing the low stretchability and flexibility of nanocellulose, induced by strong hydrogen bonds, it is still in competition with petroleum-based polymers to be used in wearable sensors.

## Declaration of Competing Interest

The authors declare that they have no known competing financial interests or personal relationships that could have appeared to influence the work reported in this paper.

## Data availability

No data was used for the research described in the article.

## Acknowledgements

This work was supported by the University of the Basque Country (Training of Researcher Staff, PIF 20/197).

## References

Aaryashree, Sahoo, S., Walke, P., Nayak, S. K., Rout, C. S., & Late, D. J. (2021). Recent developments in self-powered smart chemical sensors for wearable electronics. *Nano Research, 14*(11), 3669–3689. https://doi.org/10.1007/s12274-021-3330-8

Abbasi-Moayed, S., Golmohammadi, H., Bigdeli, A., & Hormozi-Nezhad, M. R. (2018). A rainbow ratiometric fluorescent sensor array on bacterial nanocellulose for visual discrimination of biothiols. *Analyst, 143*(14), 3415–3424. https://doi.org/10.1039/c8an00637g

Abbasi-Moayed, S., Golmohammadi, H., & Hormozi-Nezhad, M. R. (2018). A nanopaper-based artificial tongue: A ratiometric fluorescent sensor array on bacterial nanocellulose for chemical discrimination applications. *Nanoscale, 10*(5), 2492–2502. https://doi.org/10.1039/c7nr05801b

Abdalkarim, S. Y. H., Chen, L. M., Yu, H. Y., Li, F., Chen, X., Zhou, Y., & Tam, K. C. (2021). Versatile nanocellulose-based nanohybrids: A promising-new class for active packaging applications. *International Journal of Biological Macromolecules, 182*, 1915–1930. https://doi.org/10.1016/j.ijbiomac.2021.05.169

Abdi, M. M., Razalli, R. L., Tahir, P. M., Chaibakhsh, N., Hassani, M., & Mir, M. (2019). Optimized fabrication of newly cholesterol biosensor based on nanocellulose. *International Journal of Biological Macromolecules, 126*, 1213–1222. https://doi.org/10.1016/j.ijbiomac.2019.01.001

Ahmed, A., Rushworth, J. V., Hirst, N. A., & Millner, P. A. (2014). Biosensors for whole-cell bacterial detection. *Clinical Microbiology Reviews, 27*(3), 631–646. https://doi.org/10.1128/CMR.00120-13

Ali, M. A., Hu, C., Yttri, E. A., & Panat, R. (2022). Recent advances in 3D printing of biomedical sensing devices. *Advanced Functional Materials, 32*(9). https://doi.org/10.1002/adfm.202107671

Anirudhan, T. S., Deepa, J. R., & Binussreejayan. (2018). Electrochemical sensing of cholesterol by molecularly imprinted polymer of silylated graphene oxide and chemically modified nanocellulose polymer. *Materials Science and Engineering C, 92*, 942–956. https://doi.org/10.1016/j.msec.2018.07.041

Bacakova, L., Pajorova, J., Tomkova, M., Matejka, R., Broz, A., Stepanovska, J., Prazak, S., Skogberg, A., Siljander, S., & Kallio, P. (2020). Applications of

nanocellulose/nanocarbon composites: Focus on biotechnology and medicine. *Nanomaterials, 10*(2), 1–32. https://doi.org/10.3390/nano10020196
Batista, E., Angels Moncusi, M., López-Aguilar, P., Martínez-Ballesté, A., & Solanas, A. (2021). Sensors for context-aware smart healthcare: A security perspective. *Sensors, 21*(20), 1–60. https://doi.org/10.3390/s21206886
Brakat, A., & Zhu, H. (2021). Nanocellulose-graphene hybrids: advanced functional materials as multifunctional sensing platform. *Nano-Micro Letters, 13*(1). https://doi.org/10.1007/s40820-021-00627-1. Springer Singapore.
Chen, A., & Chatterjee, S. (2013). Nanomaterials based electrochemical sensors for biomedical applications. *Chemical Society Reviews, 42*(12), 5425–5438. https://doi.org/10.1039/c3cs35518g
Chen, H., Huang, J., Hao, B., Yang, B., Chen, S., Yang, G., & Xu, J. (2019). Citrate-based fluorophore-modified cellulose nanocrystals as a biocompatible fluorescent probe for detecting ferric ions and intracellular imaging. *Carbohydrate Polymers, 224*(August), Article 115198. https://doi.org/10.1016/j.carbpol.2019.115198
Chen, T., Zhang, S. H., Lin, Q. H., Wang, M. J., Yang, Z., Zhang, Y. L., Wang, F. X., & Sun, L. N. (2020). Highly sensitive and wide-detection range pressure sensor constructed on a hierarchical-structured conductive fabric as a human-machine interface. *Nanoscale, 12*(41), 21271–21279. https://doi.org/10.1039/d0nr05976e
Chen, W., & Yan, X. (2020). Progress in achieving high-performance piezoresistive and capacitive flexible pressure sensors: A review. *Journal of Materials Science and Technology, 43*, 175–188. https://doi.org/10.1016/j.jmst.2019.11.010
Chen, Y., Zhu, J., Yu, H. Y., & Li, Y. (2020). Fabricating robust soft-hard network of self-healable polyvinyl alcohol composite films with functionalized cellulose nanocrystals. *Composites Science and Technology, 194*. https://doi.org/10.1016/j.compscitech.2020.108165
Chen, Z., Yan, T., & Pan, Z. (2021). Review of flexible strain sensors based on cellulose composites for multi-faceted applications. *Cellulose, 28*(2), 615–645. https://doi.org/10.1007/s10570-020-03543-6
Choi, J. R. (2020). Development of point-of-care biosensors for COVID-19. *Frontiers in Chemistry, 8*. https://doi.org/10.3389/fchem.2020.00517
Dai, C., Liu, Y., & Wei, D. (2022). Two-dimensional field-effect transistor sensors: The road toward commercialization. *Chemical Reviews*. https://doi.org/10.1021/acs.chemrev.1c00924. acs.chemrev.1c00924.
Dai, L., Wang, Y., Zou, X., Chen, Z., Liu, H., & Ni, Y. (2020). Ultrasensitive physical, bio, and chemical sensors derived from 1-, 2-, and 3-D nanocellulosic materials. *Small, 16*(13), 1–25. https://doi.org/10.1002/smll.201906567
Dejous, C., & Krishnan, U. M. (2021). Sensors for diagnosis of prostate cancer: Looking beyond the prostate specific antigen. *Biosensors and Bioelectronics, 173*, Article 112790. https://doi.org/10.1016/J.BIOS.2020.112790
Di Nardo, F., Basili, T., Meletani, S., & Scaradozzi, D. (2022). Wavelet-based assessment of the muscle-activation frequency range by EMG analysis. *IEEE Access, 10*, 9793–9805. https://doi.org/10.1109/ACCESS.2022.3141162
Dortez, S., Sierra, T., Álvarez-Sánchez, M., González-Domínguez, J. M., Benito, A. M., Maser, W. K., Crevillen, A. G., & Escarpa, A. (2022). Effect of nanocellulose polymorphism on electrochemical analytical performance in hybrid nanocomposites with non-oxidized single-walled carbon nanotubes. *Microchimica Acta, 189*(2). https://doi.org/10.1007/s00604-021-05161-w
dos Santos, W. T. P., Amin, H. M. A., & Compton, R. G. (2019). A nano-carbon electrode optimized for adsorptive stripping voltammetry: Application to detection of the stimulant selegiline in authentic saliva. *Sensors and Actuators, B: Chemical, 279*, 433–439. https://doi.org/10.1016/j.snb.2018.10.037
Durairaj, V., Wester, N., Etula, J., Laurila, T., Lehtonen, J., Rojas, O. J., Pahimanolis, N., & Koskinen, J. (2019). Multiwalled carbon nanotubes/nanofibrillar cellulose/nafion composite-modified tetrahedral amorphous carbon electrodes for selective dopamine detection. *Journal of Physical Chemistry C, 123*(40), 24826–24836. https://doi.org/10.1021/acs.jpcc.9b05537
Fan, J., Liang, S., Zhang, M., & Xu, G. (2018). Fabrication of nanocomposite electrochemical sensors with poly(3,4-ethylenedioxythiophene) conductive polymer and Au nanoparticles adsorbed on carboxylated nanocrystalline cellulose. *Journal of Bioresources and Bioproducts, 3*(1). https://doi.org/10.21967/jbb.v3i1.142
Faham, S., Golmohammadi, H., Ghavami, R., & Khayatian, G. (2019). A nanocellulose-based colorimetric assay kit for smartphone sensing of iron and iron-chelating deferoxamine drug in biofluids. *Analytica Chimica Acta, 1087*, 104–112. https://doi.org/10.1016/j.aca.2019.08.056
Fang, S., Zhang, Z., Yang, H., Wang, G., Gu, L., Xia, L., Zeng, Z., & Zhu, L. (2020). Mussel-inspired hydrophilic modification of polypropylene membrane for oil-in-water emulsion separation. *Surface and Coatings Technology, 403*. https://doi.org/10.1016/j.surfcoat.2020.126375
Faradillawan Khalid, W. E., Nasir Mat Arip, M., Jasmani, L., & Heng Lee, Y. (2019). A new sensor for methyl paraben using an electrode made of a cellulose nanocrystal–reduced graphene oxide nanocomposite. *Sensors (Switzerland), 19*(12). https://doi.org/10.3390/s19122726
Feng, Y., Zhou, D., Gao, L., & He, F. (2020). Electrochemical biosensor for rapid detection of bacteria based on facile synthesis of silver wire across electrodes. *Biosensors and Bioelectronics, 168*. https://doi.org/10.1016/j.bios.2020.112527
Gennari, A., Führ, A. J., Volpato, G., & Volken de Souza, C. F. (2020). Magnetic cellulose: Versatile support for enzyme immobilization - a review. *Carbohydrate Polymers, 246*. https://doi.org/10.1016/j.carbpol.2020.116646
Ghasemlou, M., Daver, F., Ivanova, E. P., Habibi, Y., & Adhikari, B. (2021). Surface modifications of nanocellulose: From synthesis to high-performance nanocomposites. *Progress in Polymer Science, 119*, Article 101418. https://doi.org/10.1016/j.progpolymsci.2021.101418
Golmohammadi, H., Morales-Narváez, E., Naghdi, T., & Merkoçi, A. (2017). Nanocellulose in sensing and biosensing. *Chemistry of Materials, 29*(13), 5426–5446. https://doi.org/10.1021/acs.chemmater.7b01170
Gomes, N. O., Carrilho, E., Machado, S. A. S., & Sgobbi, L. F. (2020). Bacterial cellulose-based electrochemical sensing platform: A smart material for miniaturized biosensors. *Electrochimica Acta, 349*. https://doi.org/10.1016/j.electacta.2020.136341
Gopi, S., Balakrishnan, P., Chandradhara, D., Poovathankandy, D., & Thomas, S. (2019). General scenarios of cellulose and its use in the biomedical field. *Materials Today Chemistry, 13*, 59–78. https://doi.org/10.1016/j.mtchem.2019.04.012
Haick, H., & Tang, N. (2021). Artificial intelligence in medical sensors for clinical decisions. *ACS Nano, 15*(3), 3557–3567. https://doi.org/10.1021/acsnano.1c00085
Han, D., Yan, Y., Bian, X., Wang, J., Zhao, M., Duan, X., Kong, L., Cheng, W., & Ding, S. (2020). A novel electrochemical biosensor based on peptidoglycan and platinum-nickel-copper nano-cube for rapid detection of gram-positive bacteria. *Microchimica Acta, 187*(11), 1–10. https://doi.org/10.1007/s00604-020-04581-4
Han, J., Lu, K., Yue, Y., Mei, C., Huang, C., Wu, Q., & Xu, X. (2019). Nanocellulose-templated assembly of polyaniline in natural rubber-based hybrid elastomers toward flexible electronic conductors. *Industrial Crops and Products, 128*(June 2018), 94–107. https://doi.org/10.1016/j.indcrop.2018.11.004
He, X., Wu, C., Qian, Y., Li, Y., Zhang, L., Ding, F., Chen, H., & Shen, J. (2019). Highly sensitive and selective light-up fluorescent probe for monitoring gallium and chromium ions in vitro and in vivo. *Analyst, 144*(12), 3807–3816. https://doi.org/10.1039/c9an00625g
Hermawan, A., Amrillah, T., Riapanitra, A., Ong, W. J., & Yin, S. (2021). Prospects and challenges of MXenes as emerging sensing materials for flexible and wearable breath-based biomarker diagnosis. *Advanced Healthcare Materials, 10*(20), 1–27. https://doi.org/10.1002/adhm.202100970
Horta-Velázquez, A., & Morales-Narváez, E. (2022). Nanocellulose in wearable sensors. *Green Analytical Chemistry, 1*(February), Article 100009. https://doi.org/10.1016/j.greeac.2022.100009
Hosseini, M. S., Iraji Zad, A., Vossoughi, M., & Kalantarian, A. (2020). Development of a quartz crystal microbalance biodetector based on cellulose nanofibrils (CNFs) for glycine. *Journal of Materials Science: Materials in Electronics, 31*(20), 17451–17460. https://doi.org/10.1007/s10854-020-04301-x
Hu, B., Pu, H., & Sun, D. W. (2021). Multifunctional cellulose based substrates for SERS smart sensing: Principles, applications and emerging trends for food safety detection. *Trends in Food Science and Technology, 110*(February), 304–320. https://doi.org/10.1016/j.tifs.2021.02.005
Hu, H., Wu, X., Wang, H., Wang, H., & Zhou, J. (2019). Photo-reduction of ag nanoparticles by using cellulose-based micelles as soft templates: Catalytic and antimicrobial activities. *Carbohydrate Polymers, 213*, 419–427. https://doi.org/10.1016/j.carbpol.2019.02.062
Huang, J., Zhao, M., Hao, Y., & Wei, Q. (2022). Recent advances in functional bacterial cellulose for wearable physical sensing applications. *Advanced Materials Technologies, 7*(1), 1–14. https://doi.org/10.1002/admt.202100617
Javaid, M., Haleem, A., Rab, S., Pratap Singh, R., & Suman, R. (2021). Sensors for daily life: A review. *Sensors International, 2*(July), Article 100121. https://doi.org/10.1016/j.sintl.2021.100121
Jiang, Z., Feng, B., Xu, J., Qing, T., Zhang, P., & Qing, Z. (2020). Graphene biosensors for bacterial and viral pathogens. *Biosensors and Bioelectronics, 166*. https://doi.org/10.1016/j.bios.2020.112471
Jung, M., Kim, K., Kim, B., Lee, K. J., Kang, J. W., & Jeon, S. (2017). Vertically stacked nanocellulose tactile sensor. *Nanoscale, 9*(44), 17212–17219. https://doi.org/10.1039/c7nr03685j
Kamel, S., & Khattab, T. A. (2020). Recent advances in cellulose-based biosensors for medical diagnosis. *Biosensors, 10*(6), 67. https://doi.org/10.3390/BIOS10060067
Kang, B. H., Park, K., Hambsch, M., Hong, S., Kim, H. T., Choi, D. H., Lee, J. H., Kim, S., & Kim, H. J. (2022). Skin-conformable photoplethysmogram sensors for energy-efficient always-on cardiovascular monitoring systems. *Nano Energy, 92*(August 2021), Article 106773. https://doi.org/10.1016/j.nanoen.2021.106773
Karuk Elmas, S. N., Dincer, Z. E., Erturk, A. S., Bostanci, A., Karagoz, A., Koca, M., Sadi, G., & Yilmaz, I. (2020). A novel fluorescent probe based on isocoumarin for Hg2+ and Fe3+ ions and its application in live-cell imaging. *Spectrochimica Acta - Part A: Molecular and Biomolecular Spectroscopy, 224*, Article 117402. https://doi.org/10.1016/j.saa.2019.117402
Khalid, W. E. F. W., Heng, L. Y., & Arip, M. N. M. (2018). Surface modification of cellulose nanomaterial for urea biosensor application. *Sains Malaysiana, 47*(5), 941–949. https://doi.org/10.17576/jsm-2018-4705-09
Khalilzadeh, M. A., Tajik, S., Beitollahi, H., & Venditti, R. A. (2020). Green synthesis of magnetic nanocomposite with iron oxide deposited on cellulose nanocrystals with copper (Fe3O4@CNC/Cu): Investigation of catalytic activity for the development of a venlafaxine electrochemical sensor. *Industrial and Engineering Chemistry Research, 59*(10), 4219–4228. https://doi.org/10.1021/acs.iecr.9b06214
Khan, M. Z. H., Hasan, M. R., Hossain, S. I., Ahommed, M. S., & Daizy, M. (2020). Ultrasensitive detection of pathogenic viruses with electrochemical biosensor: State of the art. *Biosensors and Bioelectronics, 166*(April), Article 112431. https://doi.org/10.1016/j.bios.2020.112431
Khattab, T. A., Dacrory, S., Abou-Yousef, H., & Kamel, S. (2019). Smart microfibrillated cellulose as swab sponge-like aerogel for real-time colorimetric naked-eye sweat monitoring. *Talanta, 205*. https://doi.org/10.1016/j.talanta.2019.120166
Khattab, T. A., Fouda, M. M. G., Allam, A. A., Othman, S. I., Bin-Jumah, M., Al-Harbi, H. M., & Rehan, M. (2018). Selective colorimetric detection of fe (III) using metallochromic tannin-impregnated silica strips. *ChemistrySelect, 3*(43), 12065–12071. https://doi.org/10.1002/slct.201802506
Khattab, T. A., Fouda, M. M. G., Rehan, M., Okla, M. K., Alamri, S. A., Alaraidh, I. A., AL-ghamdi, A. A., Soufan, W. H., Abdelsalam, E. M., & Allam, A. A. (2020). Novel halochromic cellulose nanowhiskers from rice straw: Visual detection of urea. *Carbohydrate Polymers, 231*. https://doi.org/10.1016/j.carbpol.2019.115740

Kim, J. W., Park, H., Lee, G., Jeong, Y. R., Hong, S. Y., Keum, K., Yoon, J., Kim, M. S., & Ha, J. S. (2019). Paper-like, thin, foldable, and self-healable electronics based on PVA/CNC nanocomposite film. *Advanced Functional Materials, 29*(50). https://doi.org/10.1002/adfm.201905968

Kim, T., Bao, C., Hausmann, M., Siqueira, G., Zimmermann, T., & Kim, W. S. (2019). 3D printed disposable wireless ion sensors with biocompatible cellulose composites. *Advanced Electronic Materials, 5*(2). https://doi.org/10.1002/aelm.201800778

Klemm, D., Petzold-Welcke, K., Kramer, F., Richter, T., Raddatz, V., Fried, W., Nietzsche, S., Bellmann, T., & Fischer, D. (2021). Biotech nanocellulose: A review on progress in product design and today's state of technical and medical applications. *Carbohydrate Polymers, 254*, Article 117313. https://doi.org/10.1016/j.carbpol.2020.117313

Kramar, A., & González-Benito, F. J. (2022). Cellulose-based nanofibers processing techniques and methods based on bottom-up Approach—A review. *Polymers, 14*(2). https://doi.org/10.3390/polym14020286

Kumar, R., Rai, B., Gahlyan, S., & Kumar, G. (2021). A comprehensive review on production, surface modification and characterization of nanocellulose derived from biomass and its commercial applications. *Express Polymer Letters, 15*(2), 104–120. https://doi.org/10.3144/expresspolymlett.2021.11

Lesani, P., Singh, G., Viray, C. M., Ramaswamy, Y., Zhu, D. M., Kingshott, P., Lu, Z., & Zreiqat, H. (2020). Two-photon dual-emissive carbon dot-based probe: Deep-tissue imaging and ultrasensitive sensing of intracellular ferric ions. *ACS Applied Materials and Interfaces, 12*(16), 18395–18406. https://doi.org/10.1021/acsami.0c05217

Li, B., Mei, H., Chang, Y., Xu, K., & Yang, L. (2020). A novel near-infrared turn-on fluorescent probe for the detection of Fe3+ and Al3+ and its applications in living cells imaging. *Spectrochimica Acta - Part A: Molecular and Biomolecular Spectroscopy, 239*, Article 118552. https://doi.org/10.1016/j.saa.2020.118552

Li, G., Sun, K., Li, D., Lv, P., Wang, Q., Huang, F., & Wei, Q. (2016). Biosensor based on bacterial cellulose-au nanoparticles electrode modified with laccase for hydroquinone detection. *Colloids and Surfaces A: Physicochemical and Engineering Aspects, 509*, 408–414. https://doi.org/10.1016/j.colsurfa.2016.09.028

Li, X., Feng, Q., Lu, K., Huang, J., Zhang, Y., Hou, Y., Qiao, H., Li, D., & Wei, Q. (2021). Encapsulating enzyme into metal-organic framework during in-situ growth on cellulose acetate nanofibers as self-powered glucose biosensor. *Biosensors and Bioelectronics, 171*. https://doi.org/10.1016/j.bios.2020.112690

Lin, K. C., Muthukumar, S., & Prasad, S. (2020). Flex-GO (Flexible graphene oxide) sensor for electrochemical monitoring lactate in low-volume passive perspired human sweat. *Talanta, 214*. https://doi.org/10.1016/j.talanta.2020.120810

Liu, D. Y., Sui, G. X., & Bhattacharyya, D. (2014). Synthesis and characterisation of nanocellulose-based polyaniline conducting films. *Composites Science and Technology, 99*, 31–36. https://doi.org/10.1016/j.compscitech.2014.05.001

Liu, J., Bao, S., & Wang, X. (2022). Applications of graphene-based materials in sensors: A review. *Micromachines, 13*(2). https://doi.org/10.3390/mi13020184

Liu, J., Ji, H., Lv, X., Zeng, C., Li, H., Li, F., Qu, B., Cui, F., & Zhou, Q. (2022). Laser-induced graphene (LIG)-driven medical sensors for health monitoring and diseases diagnosis. *Microchimica Acta, 189*(2). https://doi.org/10.1007/s00604-021-05157-6

Lu, J., Han, X., Dai, L., Li, C., Wang, J., Zhong, Y., Yu, F., & Si, C. (2020). Conductive cellulose nanofibrils-reinforced hydrogels with synergetic strength, toughness, self-adhesion, flexibility and adjustable strain responsiveness. *Carbohydrate Polymers, 250*. https://doi.org/10.1016/j.carbpol.2020.117010

Lu, S., Ma, T., Hu, X., Zhao, J., Liao, X., Song, Y., & Hu, X. (2022). Facile extraction and characterization of cellulose nanocrystals from agricultural waste sugarcane straw. *Journal of the Science of Food and Agriculture, 102*(1), 312–321. https://doi.org/10.1002/jsfa.11360

Mahmoud, A. M., Mahnashi, M. H., Alkahtani, S. A., & El-Wekil, M. M. (2020). Nitrogen and sulfur co-doped graphene quantum dots/nanocellulose nanohybrid for electrochemical sensing of anti-schizophrenic drug olanzapine in pharmaceuticals and human biological fluids. *International Journal of Biological Macromolecules, 165*, 2030–2037. https://doi.org/10.1016/j.ijbiomac.2020.10.084

Mandpe, P., Prabhakar, B., Gupta, H., & Shende, P. (2020). Glucose oxidase-based biosensor for glucose detection from biological fluids. *Sensor Review, 40*(4), 497–511. https://doi.org/10.1108/SR-01-2019-0017

Mbunge, E., Muchemwa, B., Jiyane, S., & Batani, J. (2021). Sensors and healthcare 5.0: Transformative shift in virtual care through emerging digital health technologies. *Global Health Journal, 5*(4), 169–177. https://doi.org/10.1016/j.glohj.2021.11.008

Misra, R., Acharya, S., Sushmitha, & Nehru. (2021). *Nanobiosensor-based Diagnostic Tools in Viral Infections: Special Emphasis on Covid-19*. https://doi.org/10.1002/rmv.2267

Mohankumar, P., Ajayan, J., Mohanraj, T., & Yasodharan, R. (2021). Recent developments in biosensors for healthcare and biomedical applications: A review. *Measurement: Journal of the International Measurement Confederation, 167*(July 2020). https://doi.org/10.1016/j.measurement.2020.108293

Mugo, S. M., & Alberkant, J. (2020). Flexible molecularly imprinted electrochemical sensor for cortisol monitoring in sweat. *Analytical and Bioanalytical Chemistry, 412*(8), 1825–1833. https://doi.org/10.1007/s00216-020-02430-0

Nadporozhskaya, M., Kovsh, N., Paolesse, R., & Lvova, L. (2022). Recent advances in chemical sensors for soil analysis: A review. *Chemosensors, 10*(1). https://doi.org/10.3390/chemosensors10010035

Nagarajan, K. J., Ramanujam, N. R., Sanjay, M. R., Siengchin, S., Surya Rajan, B., Sathick Basha, K., Madhu, P., & Raghav, G. R. (2021). A comprehensive review on cellulose nanocrystals and cellulose nanofibers: Pretreatment, preparation, and characterization. *Polymer Composites, 42*(4). https://doi.org/10.1002/pc.25929

Nagraik, R., Sharma, A., Kumar, D., Mukherjee, S., Sen, F., & Kumar, A. P. (2021). Amalgamation of biosensors and nanotechnology in disease diagnosis: Mini-review. *Sensors International, 2*(March), Article 100089. https://doi.org/10.1016/j.sintl.2021.100089

Narwal, V., Deswal, R., Batra, B., Kalra, V., Hooda, R., Sharma, M., & Rana, J. S. (2019). Cholesterol biosensors: A review. *Steroids, 143*, 6–17. https://doi.org/10.1016/j.steroids.2018.12.003

Nath, J., Saikia, P. P., Handique, J., Gupta, K., & Dolui, S. K. (2020). Multifunctional mussel-inspired gelatin and tannic acid-based hydrogel with pH-controllable release of vitamin B12. *Journal of Applied Polymer Science, 137*(39). https://doi.org/10.1002/app.49193

Nehra, P., & Chauhan, R. P. (2021). Eco-friendly nanocellulose and its biomedical applications: Current status and future prospect. *Journal of Biomaterials Science, Polymer Edition, 32*(1), 112–149. https://doi.org/10.1080/09205063.2020.1817706

Neubauerova, K., Carneiro, M. C. C. G., Rodrigues, L. R., Moreira, F. T. C., & Sales, M. G. F. (2020). Nanocellulose- based biosensor for colorimetric detection of glucose. *Sensing and Bio-Sensing Research, 29*(July), Article 100368. https://doi.org/10.1016/j.sbsr.2020.100368

Nguyen, L. H., Naficy, S., Chandrawati, R., & Dehghani, F. (2019). Nanocellulose for sensing applications. *Advanced Materials Interfaces, 6*(18), 30–33. https://doi.org/10.1002/admi.201900424

Noor Masidayu Sayed Is, S., Zainab Ibrahim, S., & Azlina Ab. Aziz, N. (2022). A comparison of emotion recognition system using electrocardiogram (ECG) and photoplethysmogram (PPG). *Journal of King Saud University - Computer and Information Sciences, xxxx*. https://doi.org/10.1016/j.jksuci.2022.04.012

Nsabimana, A., Ma, X., Yuan, F., Du, F., Abdussalam, A., Lou, B., & Xu, G. (2019). Nanomaterials-based electrochemical sensing of cardiac biomarkers for acute myocardial infarction: Recent Progress. *Electroanalysis, 31*(2), 177–187. https://doi.org/10.1002/elan.201800641

Nwosu, F. O., Saliu, O. D., Oyinlola, K. A., & Ojo, E. O. (2020). Colorimetric based polysorbate crosslinked cellulose-Ag–Cu nanohybrid sensor for urea sensing applications. *Journal of Polymers and the Environment, 28*(5), 1475–1483. https://doi.org/10.1007/s10924-020-01703-0

Omran, A. A. B., Mohammed, A. A. B. A., Sapuan, S. M., Ilyas, R. A., Asyraf, M. R. M., Koloor, S. S. R., & Petrů, M. (2021). Micro-and nanocellulose in polymer composite materials: A review. *Polymers, 13*(2), 1–30. https://doi.org/10.3390/polym13020231

Oprea, M., & Voicu, S. I. (2020). Recent advances in composites based on cellulose derivatives for biomedical applications. *Carbohydrate Polymers, 247*. https://doi.org/10.1016/j.carbpol.2020.116683

Özbek, O., Berkel, C., & Isildak, Ö. (2020). Applications of potentiometric sensors for the determination of drug molecules in biological samples. *Critical Reviews in Analytical Chemistry*. https://doi.org/10.1080/10408347.2020.1825065

Panigrahi, P., Sajjad, M., Singh, D., Hussain, T., Andreas Larsson, J., Ahuja, R., & Singh, N. (2022). Two-dimensional nitrogenated holey graphene (C2N) monolayer based glucose sensor for diabetes mellitus. *Applied Surface Science, 573*(August 2021), Article 151579. https://doi.org/10.1016/j.apsusc.2021.151579

Patil, T. V., Patel, D. K., Dutta, S. D., Ganguly, K., Santra, T. S., & Lim, K. T. (2022). Nanocellulose, a versatile platform: From the delivery of active molecules to tissue engineering applications. *Bioactive Materials, 9*(June 2021), 566–589. https://doi.org/10.1016/j.bioactmat.2021.07.006

Pradhan, D., Jaiswal, A. K., & Jaiswal, S. (2022). Emerging technologies for the production of nanocellulose from lignocellulosic biomass. *Carbohydrate Polymers, 285*(January), Article 119258. https://doi.org/10.1016/j.carbpol.2022.119258

Ragazzini, I., Gualandi, I., Selli, S., Polizzi, C., Cassani, M. C., Nanni, D., Gambassi, F., Tarterini, F., Tonelli, D., Scavetta, E., & Ballarin, B. (2021). A simple and industrially scalable method for making a PANI-modified cellulose touch sensor. *Carbohydrate Polymers, 254*. https://doi.org/10.1016/j.carbpol.2020.117304

Ranjbar, S., & Shahrokhian, S. (2018). Design and fabrication of an electrochemical aptasensor using au nanoparticles/carbon nanoparticles/cellulose nanofibers nanocomposite for rapid and sensitive detection of Staphylococcus aureus. *Bioelectrochemistry, 123*, 70–76. https://doi.org/10.1016/j.bioelechem.2018.04.018

Ratajczak, K., & Stobiecka, M. (2020). High-performance modified cellulose paper-based biosensors for medical diagnostics and early cancer screening: A concise review. *Carbohydrate Polymers, 229*(October 2019). https://doi.org/10.1016/j.carbpol.2019.115463

Ravichandiran, P., Boguszewska-Czubara, A., Masłyk, M., Bella, A. P., Johnson, P. M., Subramaniyan, S. A., Shim, K. S., & Yoo, D. J. (2020). A phenoxazine-based fluorescent chemosensor for dual channel detection of Cd2+ and CN− ions and its application to bio-imaging in live cells and zebrafish. *Dyes and Pigments, 172*. https://doi.org/10.1016/j.dyepig.2019.107828

Rebelo, A. R., Liu, C., Schäfer, K. H., Saumer, M., Yang, G., & Liu, Y. (2019). Poly(4-vinylaniline)/Polyaniline bilayer-functionalized bacterial cellulose for flexible electrochemical biosensors. *Langmuir, 35*(32), 10354–10366. https://doi.org/10.1021/acs.langmuir.9b01425

Reshmy, R., Philip, E., Paul, S. A., Madhavan, A., Sindhu, R., Binod, P., Pandey, A., & Sirohi, R. (2020). Nanocellulose-based products for sustainable applications-recent trends and possibilities. *Reviews in Environmental Science and Biotechnology, 19*(4), 779–806. https://doi.org/10.1007/s11157-020-09551-z

Riu, J., & Giussani, B. (2020). Electrochemical biosensors for the detection of pathogenic bacteria in food. *TrAC - Trends in Analytical Chemistry, 126*. https://doi.org/10.1016/j.trac.2020.115863

Ruiz-Palomero, C., Soriano, M. L., Benítez-Martínez, S., & Valcárcel, M. (2017). Photoluminescent sensing hydrogel platform based on the combination of nanocellulose and S, N-codoped graphene quantum dots. *Sensors and Actuators, B: Chemical, 245*, 946–953. https://doi.org/10.1016/j.snb.2017.02.006

Ruiz-Palomero, C., Soriano, M. L., & Valcárcel, M. (2016). Gels based on nanocellulose with photosensitive ruthenium bipyridine moieties as sensors for silver nanoparticles in real samples. *Sensors and Actuators, B: Chemical, 229*, 31–37. https://doi.org/10.1016/j.snb.2016.01.098

Sabry, F., Eltaras, T., Labda, W., Hamza, F., Alzoubi, K., & Malluhi, Q. (2022). Towards on-device dehydration monitoring using machine learning from wearable Device's data. *Sensors, 22*(5), 1–20. https://doi.org/10.3390/s22051887

Saikia, A., & Karak, N. (2020). Cellulose nanofiber-polyaniline nanofiber-carbon dot nanohybrid and its nanocomposite with sorbitol based hyperbranched epoxy: Physical, thermal, biological and sensing properties. *Colloids and Surfaces A: Physicochemical and Engineering Aspects, 584*. https://doi.org/10.1016/j.colsurfa.2019.124049

Sandys, V., Edwards, C., McAleese, P., O'Hare, E., & O'Seaghdha, C. (2022). Protocol of a pilot-scale, single-arm, observational study to assess the utility and acceptability of a wearable hydration monitor in haemodialysis patients. *Pilot and Feasibility Studies, 8*(1), 1–9. https://doi.org/10.1186/s40814-022-00976-7

Sang, M., Kang, K., Zhang, Y., Zhang, H., Kim, K., Cho, M., Shin, J., Hong, J. H., Kim, T., Lee, S. K., Yeo, W. H., Lee, J. W., Lee, T., Xu, B., & Yu, K. J. (2022). Ultrahigh sensitive au-doped silicon nanomembrane based wearable sensor arrays for continuous skin temperature monitoring with high precision. *Advanced Materials, 34*(4). https://doi.org/10.1002/adma.202105865

Saylan, Y., Göktürk, Ilgım, Pospiskova, K., Safarik, I., & Denizli, A. (2020). Magnetic bacterial cellulose nanofibers for nucleoside recognition. *Cellulose, 27*(16), 9479–9492. https://doi.org/10.1007/s10570-020-03425-x

Sha, R., & Badhulika, S. (n.d.). Recent advancements in fabrication of nanomaterial based biosensors for diagnosis of ovarian cancer: A comprehensive review. doi: 10.1007/s00604-020-4152-8.

Shalauddin, M., Akhter, S., Basirun, W. J., Bagheri, S., Anuar, N. S., & Johan, M. R. (2019). Hybrid nanocellulose/f-MWCNTs nanocomposite for the electrochemical sensing of diclofenac sodium in pharmaceutical drugs and biological fluids. *Electrochimica Acta, 304*, 323–333. https://doi.org/10.1016/j.electacta.2019.03.003

Shao, B., & Xiao, Z. (2020). Recent achievements in exosomal biomarkers detection by nanomaterials-based optical biosensors - A review. *Analytica Chimica Acta, 1114*, 74–84. https://doi.org/10.1016/j.aca.2020.02.041

Sharma, A., Singh, R., Singh, Y., & Sharma, A. (2022). Heart rate and blood pressure measurement based on photoplethysmogram signal using fast fourier transform ✩. *Computers and Electrical Engineering, 101*(December 2021), Article 108057. https://doi.org/10.1016/j.compeleceng.2022.108057

Shi, Z., Li, S., Li, M., Gan, L., & Huang, J. (2021). Surface modification of cellulose nanocrystals towards new materials development. *Journal of Applied Polymer Science, 138*(48). https://doi.org/10.1002/app.51555

Song, J., & Rojas, O. J. (2013). Approaching super-hydrophobicity from cellulosic materials: A review. *Nordic Pulp and Paper Research Journal, 28*(2), 216–238. https://doi.org/10.3183/npprj-2013-28-02-p216-238

Song, M., Yu, H., Zhu, J., Ouyang, Z., Abdalkarim, S. Y. H., Tam, K. C., & Li, Y. (2020). Constructing stimuli-free self-healing, robust and ultrasensitive biocompatible hydrogel sensors with conductive cellulose nanocrystals. *Chemical Engineering Journal, 398*. https://doi.org/10.1016/j.cej.2020.125547

Soriano, M. L., & Dueñas-Mas, M. J. (2018). In *Promising Sensing Platforms Based on Nanocellulose* (pp. 273–301). https://doi.org/10.1007/5346_2018_26

Stankoski, S., Kiprijanovska, I., Mavridou, I., Nduka, C., Gjoreski, H., & Gjoreski, M. (2022). Breathing rate estimation from head-worn photoplethysmography sensor data using machine learning. *Sensors, 22*(6). https://doi.org/10.3390/s22062079

Steckl, A. J., & Ray, P. (2018). Stress biomarkers in biological fluids and their point-of-use detection. *ACS Sensors, 3*(10), 2025–2044. https://doi.org/10.1021/acssensors.8b00726

Su, J., Zhang, L., Wan, C., Deng, Z., Wei, S., Yong, K. T., & Wu, Y. (2022). Dual-network self-healing hydrogels composed of graphene oxide@nanocellulose and poly(AAm-co-AAc). *Carbohydrate Polymers, 296*(April), 1–9. https://doi.org/10.1016/j.carbpol.2022.119905

Subhedar, A., Bhadauria, S., Ahankari, S., & Kargarzadeh, H. (2021). Nanocellulose in biomedical and biosensing applications: A review. In. *International Journal of Biological Macromolecules, 166*, 587–600. https://doi.org/10.1016/j.ijbiomac.2020.10.217

Supian, M. A. F., Amin, K. N. M., Jamari, S. S., & Mohamad, S. (2020). Production of cellulose nanofiber (CNF) from empty fruit bunch (EFB) via mechanical method. *Journal of Environmental Chemical Engineering, 8*(1), Article 103024. https://doi.org/10.1016/j.jece.2019.103024

Syrový, T., Maronová, S., Kuberský, P., Ehman, N. V., Vallejos, M. E., Pretl, S., Felissia, F. E., Area, M. C., & Chinga-Carrasco, G. (2019). Wide range humidity sensors printed on biocomposite films of cellulose nanofibril and poly(ethylene glycol). *Journal of Applied Polymer Science, 136*(36). https://doi.org/10.1002/app.47920

Tabatabaee, R. S., Golmohammadi, H., & Ahmadi, S. H. (2019). Easy diagnosis of jaundice: A smartphone-based nanosensor bioplatform using photoluminescent bacterial nanopaper for point-of-care diagnosis of hyperbilirubinemia. *ACS Sensors, 4*(4), 1063–1071. https://doi.org/10.1021/acssensors.9b00275

Talantikite, M., Stimpson, T. C., Gourlay, A., Le-Gall, S., Moreau, C., Cranston, E. D., Moran-Mirabal, J. M., & Cathala, B. (2021). Bioinspired thermoresponsive xyloglucan-cellulose nanocrystal hydrogels. *Biomacromolecules, 22*(2), 743–753. https://doi.org/10.1021/acs.biomac.0c01521

Tamaddon, F., & Arab, D. (2019). Urease covalently immobilized on cotton-derived nanocellulose-dialdehyde for urea detection and urea-based multicomponent synthesis of tetrahydro-pyrazolopyridines in water. *RSC Advances, 9*(71), 41893–41902. https://doi.org/10.1039/c9ra05240b

Tang, L., Chen, W., Chen, B., Lv, R., Zheng, X., Rong, C., Lu, B., & Huang, B. (2021). Sensitive and renewable quartz crystal microbalance humidity sensor based on nitrocellulose nanocrystals. *Sensors and Actuators, B: Chemical, 327*. https://doi.org/10.1016/j.snb.2020.128944

Tang, Y., Petropoulos, K., Kurth, F., Gao, H., Migliorelli, D., Guenat, O., & Generelli, S. (2020). Screen-printed glucose sensors modified with cellulose nanocrystals (CNCs) for cell culture monitoring. *Biosensors, 10*(9). https://doi.org/10.3390/bios10090125

Tavakoli, M., Ghasemian, A., Dehghani-Firouzabadi, M. R., & Mazela, B. (2022). Cellulose and its nano-derivatives as a water-repellent and fire-resistant surface: A review. *Materials, 15*(1). https://doi.org/10.3390/ma15010082

Teodoro, K. B. R., Sanfelice, R. C., Migliorini, F. L., Pavinatto, A., Facure, M. H. M., & Correa, D. S. (2021). A review on the role and performance of cellulose nanomaterials in sensors. *ACS Sensors, 6*(7), 2473–2496. https://doi.org/10.1021/acssensors.1c00473

Teymourian, H., Parrilla, M., Sempionatto, J. R., Montiel, N. F., Barfidokht, A., Van Echelpoel, R., De Wael, K., & Wang, J. (2020). Wearable electrochemical sensors for the monitoring and screening of drugs. *ACS Sensors, 5*(9), 2679–2700. https://doi.org/10.1021/acssensors.0c01318

Tian, W., Wan, C., Yong, K. T., Liu, S., Wei, S., Zhang, C., Liu, X., Su, J., Cheng, W., & Wu, Y. (2022). Learning from nature: Constructing a smart bionic structure for high-performance glucose sensing in human serums. *Advanced Functional Materials, 32*(1). https://doi.org/10.1002/adfm.202106958

Torres, F. G., Troncoso, O. P., Gonzales, K. N., Sari, R. M., & Gea, S. (2020a). Bacterial cellulose-based biosensors. *Medical Devices & Sensors, 3*(5). https://doi.org/10.1002/mds3.10102

Torres, F. G., Troncoso, O. P., Gonzales, K. N., Sari, R. M., & Gea, S. (2020b). Bacterial cellulose-based biosensors. *Medical Devices & Sensors, 3*(5), 1–13. https://doi.org/10.1002/mds3.10102

Tracey, C. T., Torlopov, M. A., Martakov, I. S., Vdovichenko, E. A., Zhukov, M., Krivoshapkin, P. V., Mikhaylov, V. I., & Krivoshapkina, E. F. (2020). Hybrid cellulose nanocrystal/magnetite glucose biosensors. *Carbohydrate Polymers, 247*(June), Article 116704. https://doi.org/10.1016/j.carbpol.2020.116704

Vanderfleet, O. M., & Cranston, E. D. (2021). Production routes to tailor the performance of cellulose nanocrystals. *Nature Reviews Materials, 6*(2), 124–144. https://doi.org/10.1038/s41578-020-00239-y

Varshney, S., Kumar, P., Singhal, A., & Varshney, G. (2022). Materials Today : Proceedings A review on the recent developments in the materials used for sensors. *Materials Today: Proceedings, xxxx*. https://doi.org/10.1016/j.matpr.2022.04.678

Wang, H., Luo, H., Zhou, H., Zhou, X., Zhang, X. X., Lin, W., Yi, G., & Zhang, Y. (2018). Dramatically enhanced strain- and moisture-sensitivity of bioinspired fragmentized carbon architectures regulated by cellulose nanocrystals. *Chemical Engineering Journal, 345*, 452–461. https://doi.org/10.1016/j.cej.2018.04.003

Wang, Y., Chen, Z., Mei, D., Zhu, L., Wang, S., & Fu, X. (2022). Highly sensitive and flexible tactile sensor with truncated pyramid-shaped porous graphene/silicone rubber composites for human motion detection. *Composites Science and Technology, 217*(June 2021), Article 109078. https://doi.org/10.1016/j.compscitech.2021.109078

Wang, Y., Hou, S., Li, T., Jin, S., Shao, Y., Yang, H., Wu, D., Dai, S., Lu, Y., Chen, S., & Huang, J. (2020). Flexible capacitive humidity sensors based on ionic conductive wood-derived cellulose nanopapers. *ACS Applied Materials and Interfaces, 12*(37), 41896–41904. https://doi.org/10.1021/acsami.0c12868

Wang, Y., Wang, Q., Liu, S., Ji, X., Yang, G., & Chen, J. (2022). Lipase induced highly hydrophobic nanofibrillated cellulose film for strain sensor application. *Carbohydrate Polymers, 284*. https://doi.org/10.1016/j.carbpol.2022.119193

Wang, Y., Yang, X., Pang, L., Geng, P., Mi, F., Hu, C., Peng, F., & Guan, M. (2022). Application progress of magnetic molecularly imprinted polymers chemical sensors in the detection of biomarkers. *Analyst, 147*(4), 571–586. https://doi.org/10.1039/d1an01112j

Wu, Y., Sun, S., Geng, A., Wang, L., Song, C., Xu, L., Jia, C., Shi, J., & Gan, L. (2020). Using TEMPO-oxidized-nanocellulose stabilized carbon nanotubes to make pigskin hydrogel conductive as flexible sensor and supercapacitor electrode: Inspired from a chinese cuisine. *Composites Science and Technology, 196*. https://doi.org/10.1016/j.compscitech.2020.108226

Xiang, F., Li, J., & Liu, Z. (2019). PH-dependent photoluminescence "switch-on" nanosensors composed of silver nanoparticles and nitrogen and Sulphur co-doped carbon dots for discriminative detection of biothiols. *Analyst, 144*(23), 7057–7063. https://doi.org/10.1039/c9an01488h

Yan, Q., Zhou, M., & Fu, H. (2020). Study on mussel-inspired tough TA/PANI@CNCs nanocomposite hydrogels with superior self-healing and self-adhesive properties for strain sensors. *Composites Part B: Engineering, 201*. https://doi.org/10.1016/j.compositesb.2020.108356

Yao, Y., Huang, X. H., Zhang, B. Y., Zhang, Z., Hou, D., Zhou, & Kun, Z. (2020). Facile fabrication of high sensitivity cellulose nanocrystals based QCM humidity sensors with asymmetric electrode structure. *Sens. Actuators, B: Chemical, 302*. https://doi.org/10.1016/j.snb.2019.127192

Yavuz, O., Sezen, M., Alcay, Y., Yildirim, M. S., Kaya, K., Ozkilic, Y., Tuzun, N.Ş., & Yilmaz, I. (2021). A new perspective on the beryllium sensor platform: Low symmetry phthalocyanine-based molecular design and ultra trace amount Be2+ ion recognition in aqueous media. *Sensors and Actuators, B: Chemical, 329*. https://doi.org/10.1016/j.snb.2020.129002

Yoon, J., Cho, H. Y., Shin, M., Choi, H. K., Lee, T., & Choi, J. W. (2020). Flexible electrochemical biosensors for healthcare monitoring. *Journal of Materials Chemistry B, 8*(33), 7303–7318. https://doi.org/10.1039/d0tb01325k

Yoon, J. H., Kim, S. M., Park, H. J., Kim, Y. K., Oh, D. X., Cho, H. W., Lee, K. G., Hwang, S. Y., Park, J., & Choi, B. G. (2020). Highly self-healable and flexible cable-type pH sensors for real-time monitoring of human fluids. *Biosensors and Bioelectronics, 150*. https://doi.org/10.1016/j.bios.2019.111946

Yu, Z., Hu, C., Guan, L., Zhang, W., & Gu, J. (2020). Green synthesis of cellulose nanofibrils decorated with ag nanoparticles and their application in colorimetric

detection of l -cysteine. *ACS Sustainable Chemistry and Engineering, 8*(33), 12713–12721. https://doi.org/10.1021/acssuschemeng.0c04842

Yuen, J. D., Shriver-Lake, L. C., Walper, S. A., Zabetakis, D., Breger, J. C., & Stenger, D. A. (2020). Microbial nanocellulose printed circuit boards for medical sensing. *Sensors (Switzerland), 20*(7). https://doi.org/10.3390/s20072047

Zaid, M. H. M., Abdullah, J., Yusof, N. A., Wasoh, H., Sulaiman, Y., Noh, M. F. M., & Issa, R. (2020). Reduced graphene Oxide/TEMPO-nanocellulose nanohybrid-based electrochemical biosensor for the determination of mycobacterium tuberculosis. *Journal of Sensors, 2020*. https://doi.org/10.1155/2020/4051474

Zaid, M. H. M., Che-Engku-Chik, C. E. N., Yusof, N. A., Abdullah, J., Othman, S. S., Issa, R., Md Noh, M. F., & Wasoh, H. (2020). DNA electrochemical biosensor based on iron oxide/nanocellulose crystalline composite modified screen-printed carbon electrode for detection of mycobacterium tuberculosis. *Molecules, 25*(15). https://doi.org/10.3390/molecules25153373

Zhang, J., Zhang, X., Wei, X., Xue, Y., Wan, H., & Wang, P. (2021). Recent advances in acoustic wave biosensors for the detection of disease-related biomarkers: A review. *Analytica Chimica Acta, 1164*, Article 338321. https://doi.org/10.1016/j.aca.2021.338321

Zhang, L., Lyu, S., Zhang, Q., Wu, Y., Melcher, C., Chmely, S. C., Chen, Z., & Wang, S. (2019). Dual-emitting film with cellulose nanocrystal-assisted carbon dots grafted SrAl2O4, Eu2+, Dy3+ phosphors for temperature sensing. *Carbohydrate Polymers, 206*, 767–777. https://doi.org/10.1016/j.carbpol.2018.11.031

Zhang, L., Wan, C., Su, J., Zhang, C., Wei, S., Tian, W., Liu, X., Cheng, W., Li, X., Li, X., Guo, X., Yong, K. T., & Wu, Y. (2022). A dual-crosslinked self-healing and antibacterial nanocellulose hydrogel for monitoring of human motions. *Materials and Design, 215*. https://doi.org/10.1016/j.matdes.2022.110464

Zhang, Y., Liu, G., Yao, X., Gao, S., Xie, J., Xu, H., & Lin, N. (2018). Electrochemical chiral sensor based on cellulose nanocrystals and multiwall carbon nanotubes for discrimination of tryptophan enantiomers. *Cellulose, 25*(7), 3861–3871. https://doi.org/10.1007/s10570-018-1816-1

Zhang, Z., Liu, G., Li, X., Zhang, S., Xingqiang, L., & Wang, Y. (2020). Design and synthesis of fluorescent nanocelluloses for sensing and bioimaging applications. *ChemPlusChem, 85*(3), 487–502. https://doi.org/10.1002/cplu.201900746

Zhao, J., Gong, Z., Chen, C., Liang, C., Wang, S., Huang, L., Huang, M., & Qin, C. (2022). Adsorption mechanism of chloropropanol by crystalline nanocellulose. *Polymers, 14*(9). https://doi.org/10.3390/polym14091746

Zhao, L., Jiang, Y., Hao, J., Wei, H., Zheng, W., & Mao, L. (2019). Graphdiyne oxide enhances the stability of solid contact-based ionselective electrodes for excellent in vivo analysis. *SCIENCE CHINA Chemistry, 62*(10), 1414–1420. https://doi.org/10.1007/s11426-019-9516-5

Zheng, C., Lu, K., Lu, Y., Zhu, S., Yue, Y., Xu, X., Mei, C., Xiao, H., Wu, Q., & Han, J. (2020). A stretchable, self-healing conductive hydrogels based on nanocellulose supported graphene towards wearable monitoring of human motion. *Carbohydrate Polymers, 250*. https://doi.org/10.1016/j.carbpol.2020.116905

Zheng, Y., Tang, N., Omar, R., Hu, Z., Duong, T., Wang, J., Wu, W., & Haick, H. (2021). Smart materials enabled with artificial intelligence for healthcare wearables. *Advanced Functional Materials, 31*(51). https://doi.org/10.1002/adfm.202105482

Zhu, P., Kuang, Y., Wei, Y., Li, F., Ou, H., Jiang, F., & Chen, G. (2021). Electrostatic self-assembly enabled flexible paper-based humidity sensor with high sensitivity and superior durability. *Chemical Engineering Journal, 404*, Article 127105. https://doi.org/10.1016/j.cej.2020.127105

Zhu, P., Liu, Y., Fang, Z., Kuang, Y., Zhang, Y., Peng, C., & Chen, G. (2019). Flexible and highly sensitive humidity sensor based on cellulose nanofibers and carbon nanotube composite film. *Langmuir, 35*(14), 4834–4842. https://doi.org/10.1021/acs.langmuir.8b04259

Zhu, P., Ou, H., Kuang, Y., Hao, L., Diao, J., & Chen, G. (2020). Cellulose Nanofiber/Carbon nanotube dual network-enabled humidity sensor with high sensitivity and durability. *ACS Applied Materials and Interfaces, 12*(29), 33229–33238. https://doi.org/10.1021/acsami.0c07995

Zhu, S., Sun, H., Lu, Y., Wang, S., Yue, Y., Xu, X., Mei, C., Xiao, H., Fu, Q., & Han, J. (2021). Inherently conductive Poly(dimethylsiloxane) elastomers synergistically mediated by Nanocellulose/Carbon nanotube nanohybrids toward highly sensitive, stretchable, and durable strain sensors. *ACS Applied Materials and Interfaces, 13*(49), 59142–59153. https://doi.org/10.1021/acsami.1c19482

Zhuo, H., Hu, Y., Chen, Z., Peng, X., Liu, L., Luo, Q., Yi, J., Liu, C., & Zhong, L. (2019). A carbon aerogel with super mechanical and sensing performances for wearable piezoresistive sensors. *Journal of Materials Chemistry A, 7*(14), 8092–8100. https://doi.org/10.1039/c9ta00596j